UNIVERSITY OF CRETE

Joint Graduate programme:
Molecular Biology and Biomedicine

Detection of Circulating Nucleic Acids associated with cancer using QCM-D acoustic device combined with RCA isothermal DNA amplification method

Nikoletta Naoumi

Under the supervision of:
Prof. Electra Gizeli

Acknowledgments

I would like to thank Prof. Electra Gizeli for accepting me to her laboratory and entrusting me with this project. She is a great coordinator, both in terms of supervising with her guidance and scientific knowledge and as a person as well. Her admirable trust towards to all her students were factors that made working in her lab a real pleasure. Furthermore, I would like to thank Prof. Kalantidis and Prof. Petratos, who along with Prof. Gizeli supervised this work and for their good advice.

I would also like to thank Dr. George Papadakis for his guidance, help, trust and patience during my work in the lab. His knowledge and experience have been a great help to achieve things I could not on my own. I would also like to thank Dr. Achillea Tsortos for his guidance and advice.

I would also like to thank Bodossaki Foundation for providing me a scholarship.

I want to express my gratitude to all labmates. Firstly, to Dimitra Chronaki for showing me how to use QCM biosensor and OriginPro, helping me and give me important advice plenty of times. Secondly, to Maria Megariti for her help and her friendship. Then, to Dimitra Milioni, Sofia, Aristea Grammoustianou, Alexandro Pantazi, Taso, for their cooperation and for keeping a good mood in the lab. You all have great knowledge and great personality as well!

Lastly, I would like to express my gratitude and love towards my family, Lefteris Deiktakis and all of my friends, for their unlimited support and trust!

Table of contents

Περίληψη

Ο καρκίνος αποτελεί κύρια αιτία θανάτου σε παγκόσμιο επίπεδο. Μέχρι τώρα οι κυριότερες τεχνικές που χρησιμοποιούνται για τη διάγνωση του καρκίνου είναι η ραδιολογία, η μαγνητική τομογραφία και η βιοψία με τη λήψη ιστού. Ωστόσο, οι παραπάνω μέθοδοι είναι ακριβές και απαιτούν σημαντικό χρόνο μέχρι τη λήψη των αποτελεσμάτων ενώ επίσης επιβαρύνουν την υγεία του ασθενή. Τα κυκλοφορούντα νουκλεϊκά οξέα, όπως τα κυκλοφορούν καρκινικό DNA και τα κυκλοφορούντα miRNAs έχουν χρησιμοποιηθεί επανειλημμένα για την ανάπτυξη μη επεμβατικών, μοριακών διαγνωστικών μεθόδων με στόχο την πρόγνωση και την αποτελεσματική και έγκαιρη διάγνωση του καρκίνου. Έτσι, μία μεγάλη ποικιλία μοριακών μεθόδων που βασίζονται στον πολλαπλασιασμό του στόχου, καθώς και μέθοδοι που κάνουν χρήση των νανοϋλικών, νανοτεχνολογίας και βιοαισθητήρων έχουν αναπτυχθεί ήδη. Ωστόσο, η πλειονότητα αυτών των μεθόδων χαρακτηρίζεται από υψηλό κόστος, αυξημένη πολυπλοκότητα της διαδικασίας, ενώ απαιτούν τη χρήση ειδικού εξοπλισμού και αρκετό χρόνο. Έτσι, δε δύναται να χρησιμοποιηθούν για καθημερινή κλινική εφαρμογή. Στόχος της μεταπτυχιακής διατριβής ήταν η ανάπτυξη μίας μη επεμβατικής, εύκολη στο χειρισμό και γρήγορης μεθόδου για την ανίχνευση σημειακών μεταλλάξεων στο ελεύθερο καρκινικό DNA καθώς και την ανίχνευση κυκλοφορούντων miRNAs. Και οι δύο μέθοδοι βασίζονται στη συνδυασμένη χρήση του QCM-D ακουστικού βιοαισθητήρα με την ισόθερμη μέθοδο πολλαπλασιασμού του DNA, RCA. Όσον αφορά την ανίχνευση σημειακών μεταλλάξεων στο ελεύθερο καρκινικό DNA, ανιχνεύθηκαν επιτυχώς και με υψηλή ακρίβεια τα 10 αντίγραφα του στόχου, έπειτα από την συνδυασμένη εφαρμογή αντίδραση μοριακής συγκόλλησης ακολουθούμενη από RCA. Ωστόσο, στον ακουστικό βιοαισθητήρα ανιχνεύθηκε 1 pmol του DNA στόχου. Σχετικά με την ανίχνευση κυκλοφορούντος miRNA, επιτεύχθηκε η ανίχνευση 1 fmol miRNA-21 χωρίς τη χρήση βιοαισθητήρα (off-chip), εφαρμόζοντας ενός-βήματος αντίδραση (κατά την οποία οι δύο ξεχωριστές αντιδράσεις συγκόλλησης και πολυμερισμού πραγματοποιούνται παράλληλα σε μία και μόνο αντίδραση) σε θερμοκρασία δωματίου, αποφεύγοντας τη χρήση οποιουδήποτε είδους συσκευής. Ωστόσο, το όριο ανίχνευσης στο βιοαισθητήρα αποτέλεσε το 0,1 pmol. Αν και απαιτείται η διεξαγωγή πολλών πειραμάτων ακόμη και βελτιστοποίηση των πρωτοκόλλων, τα αποτελέσματα είναι ενθαρρυντικά για την ανάπτυξη μία πρωτοπόρας διαγνωστικής μεθόδου με στίχο την κλινική εφαρμογή.

Abstract

Cancer is the leading cause of death worldwide. The gold standards of cancer diagnosis are radiology, magnetic resonance imaging (MRI) and solid biopsies. However all three methods are expensive, time-consuming and hurt the physical health of patients during the detection of cancer. Circulating tumor DNA and circulating miRNA, both cancer biomarkers, have been widely used as targets for the development of non-invasive diagnostic methods for prognosis and diagnosis of cancer. A big variety of molecular, amplification-based techniques as well as methods that utilize the advances in nanomaterilas, nanotechnology and the biosensors field have been developed, too. However, most of these methods are expensive, complex, require special instrumentation, and a lot of time, so they cannot be applicable in routine clinical practice. Herein, it was aimed the development of two non-inavnsive, easy and fast methods for the detection of ctDNA point mutations and circulating miRNAs. Both methods utilize the QCM-D acoustic biosensor, combined with the isothermal DNA amplification method, RCA. In the case of ctDNA, a minimal amount of 10 copies was detected with high specificity via Ligation followed by RCA, but only 1 pmol was managed to be detected on QCM biosensor. Concerning the second case, 1 fmol of miRNA-21 was achieved to be detected off-chip in a single-step reaction (combining the ligation and amplification step in one single step reaction) at RT, without the need of any kind of instrumentation. However, only 0.1 pmol of miRNA-21 was detected on QCM-D device. Despite both methods need a lot of further optimization, results were promising for the development of a novel detection method.

1. Introduction

Cancer is the leading cause of death worldwide. According to World health Organization there were 14 million new cases and 8.2 million cancer related deaths in 2012, and this number is predicted to rise by approximately 70% over the next two decades. The best way to achieved effective and efficient management of cancer patients is the early diagnosis and the frequent monitoring of patient response to treatment[1]. However, the gold standard of cancer diagnosis such as radiology, ultrasound scans, magnetic resonance imaging (MRI) and solid biopsies used to hurt the physical health of patients during cancer detection. Moreover, these methods are expensive and they may need a lot of time. Despite that there are cases where non-invasive cancer detection may be achieved by detecting protein biomarkers (ie. PSA and CA-125 for prostate and ovarian cancer respectively) diagnosis cannot be neither early nor effective[2,3].

The past few years, researchers have made great efforts to identify biomarkers in order to develop non-invasive diagnostics for clinical application and disease management. Nucleic acids, including DNA, mRNA and miRNAs, have enormous potential to play that role. DNA mutations, coding and non-coding RNA influence gene expression and regulation and can have disturbed expression levels across various pathological conditions including autoimmune and inflammatory diseases, cardiovascular diseases cancer etc[4].

In healthy conditions, cells release DNA and RNA in the circulation and body fluids. The so called "Liquid biopsy" based on the detection of circulating nucleic acids, seems to be an ideal method for easy and fast detection of cancer[1,5,6]. Three methods are mainly used for the detection and quantification of circulating tumor DNA and circulating miRNAs: quantitative Real Time PCR (qRT-PCR) and Reverse Transcription-quantitative PCR (RT-qPCR), microarrays and next-generation sequencing. However these methods are complex, expensive, and demand special equipment and sophisticated expertise. Advances in micro- and nano- technology as well as in biosensors field, are promising for the development of micro- fluidics, biosensing and Point-of-Care platforms applicable in daily clinical practice which would offer effective and low-cost liquid-biopsy [4,7].

1.1 Circulating tumor DNA (ctDNA)

The presence of cell-free DNA (cfDNA) in blood plasma was discovered in 1948 by Mandel and Metais. Cells and healthy tissues release DNA in the bloodstream as well as outside the blood circulation in various body fluids, including urine and saliva[8,9]. Analysis of cfDNA can give information about its origin, total amount (concentration levels) and its mutagenesis[9,10].

In healthy individuals, cfDNA concentrations tend to range from 1 to 10 ng/mL in plasma. High concentrations of cell-free DNA correlate with various pathological conditions such cancer, acute trauma and infection or physiological conditions like exercise[9]. Cancer patients have significant increased levels of cfDNA reaching even the 100 ng/mL depending from the stage of the disease. It is consider that one percentage of cfDNA is from tumor cells necrosis, ranging from 0.01% to more than 50%[5]. This percentage is increased as the disease progresses. For example the KRAS mutation

found in the plasma of pancreatic patients was identical to that found in the patient's tumour, thereby confirming that the mutant DNA fragments in the plasma were of tumor origin[9]. The half-life of cfDNA in the circulation has been determined to vary between 16 minutes and 2.5 hours due to its digestion from nucleases and filtration from liver, spleen and kidney[9,11]. Thus, ctDNA analysis is a 'real-time' snapshot of disease burden. Multiple properties of cell-free DNA suggest cell death as it major origin. However it is also released via necrosis and secretion with extracellular vesicles such as exosomes[5,9] **(Figure 1A)**. cfDNA is double-stranded and higly-frangmented with the most fragments to be 150 bp in length. Furthermore, the length of the other fragments correspond well with linear progression of nucleosome units (two units for 300 bp length, three for 450 bp)[8,9,11].

The amount of circulating tumor DNA (ctDNA) varies widely, even between patients with the same cancer type and the same stage. The levels of ctDNA tend to increase in correlation with the stage of cancer and depend of the location, size, and vascularity of the tumor[8,9,11]. Moreover, the relative levels of ctDNA within a patient have been demonstrated to correlate with the response to therapy, increasing as a tumor enlarges and decreasing with response to therapy. Patients with stage I cancer had fewer than 10 copies per 5 ml of plasma. In contrast, patients with advanced prostate, ovarian or colorectal cancer had a median concentration of 100–1,000 copies per 5 ml of plasma[9].

As mentioned before, ctDNA consider as a non-invasive "real-time" biormarker. ctDNA can provide significant information about its origin, concentration levels, DNA mutations, such as point mutations and rearrangements, epigenetic alterations, microsatellite instability, loss of heterozygosity and the number of mutated/altered alleles and can be used for diagnostic and prognostic information before, during treatment and at progression of the disease[12]. The presence of specific DNA mutations associated with tumor (usually in oncogenes or suprresor genes), reflect the patient's physical condition and the responsiveness to the treatment. ctDNA varies in different cancer types and stages of the disease as well as concerning the mutation profile between different patients[5,12] **(Figure 1B)**.

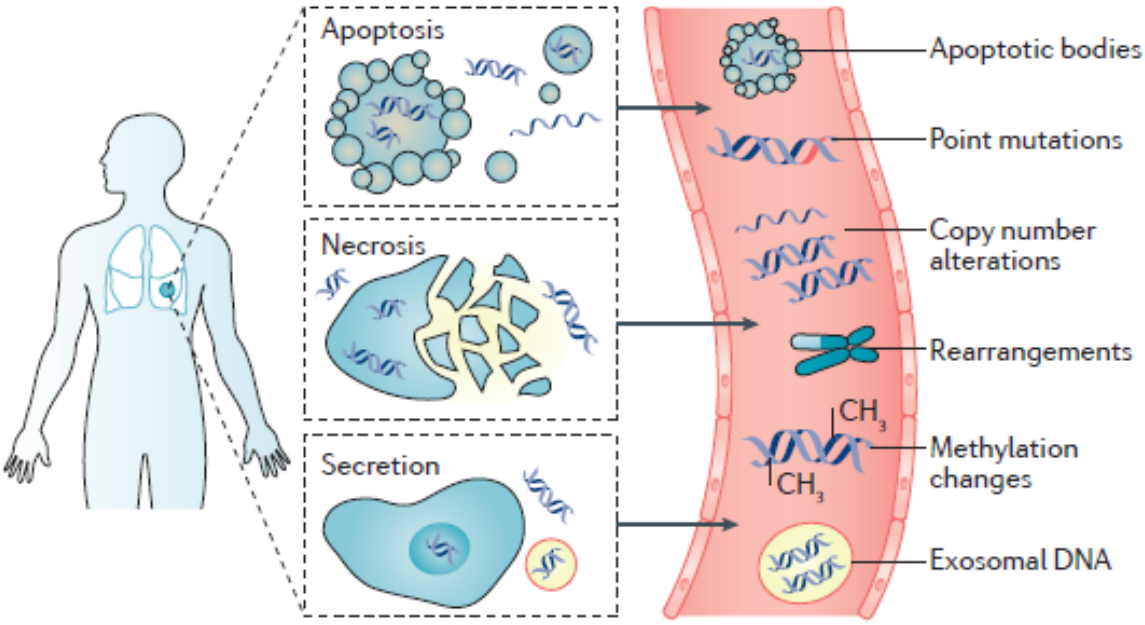

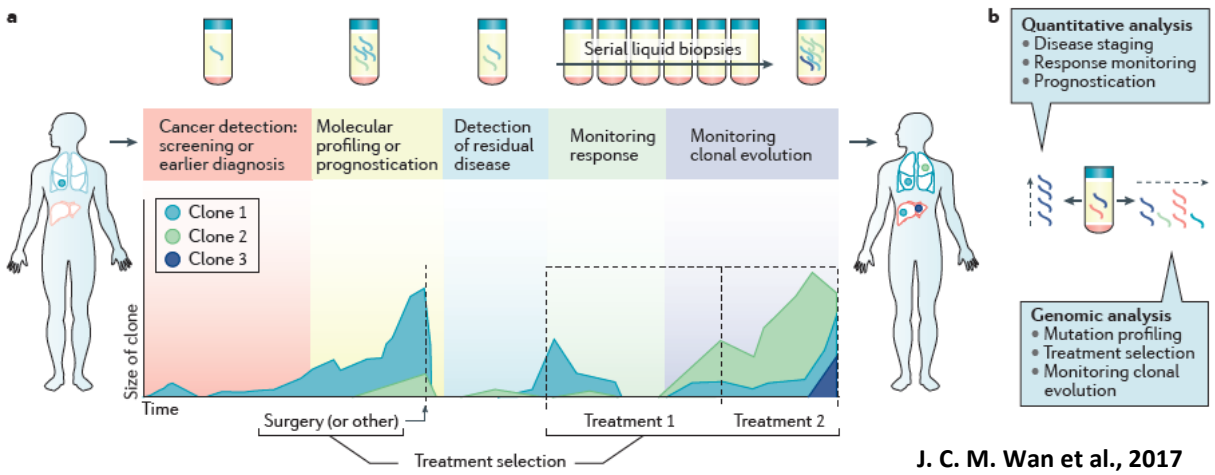

Figure 1: A) Origins and range of alterations in cell-free DNA B) Applications of ctDNA analysis during the course of disease management. a) A schematic time course for a hypothetical patient, who diagnosed with cancer, undergoes surgery (or other initial treatment), has a disease relapse and then receives systemic therapy. The potential applications of liquid biopsies for diagnosis and during this patient's care are indicated. The patient starts with one disease site, but multiple metastases and distinct clones (depicted in different colors) emerge following treatment. **b)** The information extracted from ctDNA may be classified, broadly, as quantitative information (relating to tumor burden) or genomic information. Quantification of ctDNA at a single time point may allow disease staging and prognostication, and genomic analysis can inform the selection of targeted therapies. Liquid biopsy for quantitative or genomic analysis can contribute to monitor tumor burden, treatment response, clonal evolution.

One of the major and more usual types is colorectal cancer (CRC). About 50 % of the cases with CRC are diagnosed in late stages and the 50 % of cases distant metastases. Furthermore, approximately 33 % of patients experience disease-specific mortality. There are specific mutations that were detected using ctDNA and are linked with colorectal cancer, such as in EGFR, NRAS, BRAF and KRAS genes. KRAS mutations are found in serum and plasma of the 25 % to 50 % of patients. In 2015 there was a research where it was reported the presence of KRAS G12D[6] and KRAS G13D mutation in CRC tissues in the 48 of 52 patients (92.3 %). In general it is estimated that 75 % of patients will carry at least one mutation in one of the three genes KRAS, TP53 and APC [5,10,12].

1.1.1 Amplification-based methods for the detection of ctDNA point mutations

As already stated PCR-based methods and NGS have been mainly performed for the detection of ctDNA. Cobas' ctDNA detection of EGFR mutations in lung cancer patients was the first approach that FDA approved. Cobas or Roche's PCR is a quantitative real-time PCR based method using specific primers and fluorescent probes[11,13]. Other PCR-based methods are digital-PCR (dPCR) and its variants (Droplet-Digital PCR (ddPCR) and BEAMing Digital PCR)[10,13–15], Co-amplification at Lower Denaturation temperature Polymerase Chain Reaction (COLD-PCR)[16] and Allele specific Polymerase Chain Reaction (ARMS)[13]. Digital PCR can amplify and generate many amplicons using one single copy of DNA template. Point mutations can be detected by designing specific primers. Different alleles can be distinguished either by using different fluorophores (but there limitation in multiplexing) or by sequencing of the amplicons[13,14]. During Droplet Digital-PCR DNA is fractioned

into thousands of droplets achieving single molecule isolation and each molecule is then individually analyzed. Counting the positive droplets, quantification of initial target can be achieved[13–15].

Concerning the BEAMing (beads, emulsions, amplification and magnetics) method it is based on single-molecule PCR using beads coated with thousands of primer copies for the single DNA molecule originally present, and a high number of beads are then analyzed with flow cytometry. This method has great sensitivity and can be multiplexed, for the simultaneous detection of known point mutations[10,13]. COLD-PCR methods such as full-, fast-, ice- (improved and complete enrichment) make use of a critical temperature in during PCR in order to selectively denature the wild-type-mutant heteroduplexes, allowing the enrichment of rare mutations. COLD-PCR can be combined with other technologies for the detection and/or identification of the mutation of interest like sequencing (i.e. Ion Torrent)[16]. Another PCR method, ARMS method, is using sequence specific primers, designed appropriately to detect known point mutations and leads to specific enrichment of only the mutated allele[13]. On the other hand, the more common NGS-based methods are Massive Parallel Sequencing, Whole Genome Sequencing and Whole Exome Sequencing differing in the range and the depth of sequencing[12,13].

Table 1: Comparison of PCR-based methods & NGS that have been applied for the detection of ctDNA point mutations

	PCR-based methods				NGS[10,13]
	Cobas' or Roches' PCR[13]	Droplet Digital PCR[13–15]	BEAMing Digital PCR[13,14]	ARMS[13]	
Advantages	Real time PCR	Fractionated sample	Single-molecule PCR with Magnetic beads	Qualitative	Quantitative
	Use of fluorescent probes	Absolute quantification	Absolute quantification	Use of fluorescent probes	
	Quantitative/Qualitative	Extereme Specificity (1 copy/100000)	High specificity	High Specificity	Identification of new sequenses and mutations
	Sensitive (100 copies/mL)	Extreme sensitivity	High sensitivity	Sensitive	Sensitive
	Applied in Plasma/Serum*				
		>1 day		>1day	
Disadvantages	Detects only known mutation				Time consuming (8-10 days)
	Need of specific instrumentation				
	Bioinformatics analysis				
	Time-consuming (1 day)		Analyzed by flow cytometry	Not quantitative	High cost/Expertise
	Does not give absolute quantification		Time-consuming (7-8 days)		Sophisticated statistics

*Commercially available kits were used for the extraction of cfDNA from plasma or serum, prior to any detection method

Two other methods that have not been used for the detection of ctDNA but have great sensitivity and have been applied for the detection of point mutations are Ligase Chain Reaction (LCR)[17,18] and Rolling Circle Amplification (RCA)[19–21]. LCR, like PCR require the use of multiple temperatures and thermal cycling. RCA is an isothermal DNA amplification method that it will be described later. Both methods are very good for the detection of SNPs. SNPs detection is achieved using appropriate padlock probes and a DNA ligase. Only when there is no mismatch, ligation occurs producing a template for DNA polymerase. LCR and RCA are much more specific methods than PCR for the

detection of known point mutations and can achieve a very low limit of detection, down to aM levels[20,22]. Compare to other two methods, and as it will be described later, they are more simple, include fewer steps, and cost-effective. (d)dPCR has increased analytical power, high specificity and sensitivity, allowing the detection of one mutated copy per 100.000 wild type copies[14]. Compare to the NGS-based methods, it is more cost-effective. However, it is still expensive to be performed in clinical assays; requires specific instruments for thermal cycling, is based on fluorescence measurement or sequencing, is time-consuming and needs sophisticated statics/bioinformatics analysis-tools (normalization). As concern NGS-based technologies, the only advantage is the identification of new point mutations.

1.2 Circulating miRNAs

miRNAs are endogenous small non-coding RNA molecules of 18-24 nt length, able to negatively regulate the expression of target mRNAs by partially hybridizing to their 3' untranslated region (UTR). They are transcribed from intergenic genomic sequences or intronic regions of protein-coding genes mainly by RNA polymerase II. Firstly, a long stem-loop precursor is produced (pri-miRNAs) which is subsequently processed by Drosha, a ribonuclease III enzyme producing the pre-miRNAs, molecules of approximately 70-120 nt long with a harpin-like structure. Pre-miRNAs are then recognized by exportin-5, a nuclear export factor, and transferred into the cytoplasm where they are further cleaved into duplexes of 18-24 nt by Dicer. The one (passenger) strand of the duplex is then degraded and the other strand of mature miRNA incorporates with Argonaute proteins or lipoproteins forming the RNA-induced silencing complexers (RISC)[1,23,24].

miRNAs play key role by regulating various cellular processes such as development, proliferation, differentiation, apoptosis, cell death and tumorgenesis[23–25]. Most of the miRNAs are found inside the cell. However, miRNAs are also present in various body fluids including blood, saliva, urine, tears, pleural fluid, gastric juices etc [1,23–26]. Remarkably, the presences of RNases in the circulation does not affect their stability. Instead, they are extremely resistant to various conditions, like freezing, thawing, enzymatic degradation and extreme pH [23,27]. Their expression levels are significantly altered during many diseases including cancer. The stability of miRNAs is directly connected with the way that they released outside the cell in the different biological fluids. Except from their passive release upon tissue injury, cell apoptosis and necrosis, miRNAs are also incorporated into microvesicles or exosomes followed by release in the extracellular space. However only a small part of circulating miRNA is released and found in small vesicles. The largest amount of circulating miRNA is released incorporated with RNA-binding proteins (through an RNA-binding protein dependent pathway) such as Argonaute-2 (AGO-2), high density Lipoprotein (HDL) and nucleophosmin (NPM1) [1,23,24] **(Figure 2)**.

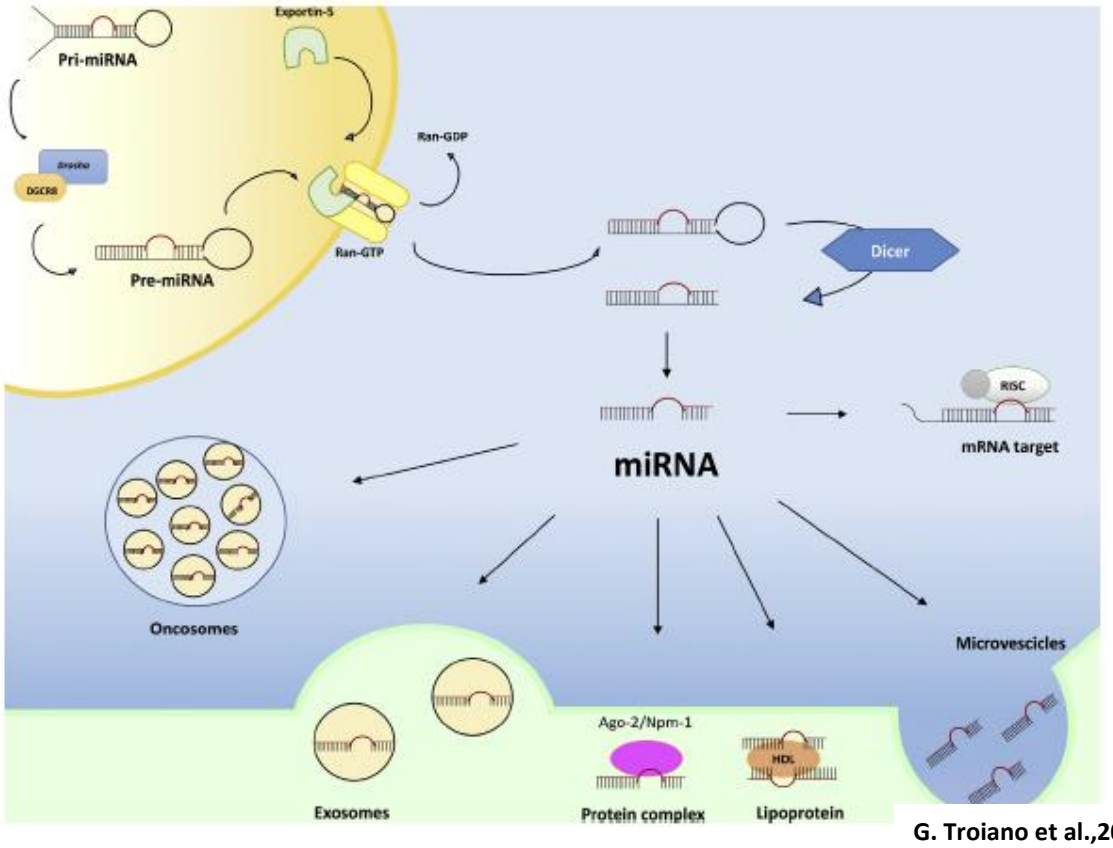

G. Troiano et al.,2016

Figure 2: Schematic representation of miRNA processing and secretion in extracellular space.

1.2.1 Circulating miRNAs in oncogenesis and other diseases

Aberrant expression of miRNAs and altered levels in the circulation have been observed in many pathological conditions including cancer[1,24,25], diabetes mellitus[26], cardiovascular[26,28] and autoimmune diseases[29] as well as during infectious diseases (viral or not)[30,31]. Their discovery in body fluids, makes them a potential source to be used as cancer biomarkers. Dysregulated expression of miRNAs have been found in every type of cancer, such as prostate, ovarian, liver, lung, oral, colorectal[1,25,32] etc. It is speculated that there is specific signature of dysregulated miRNA corresponding to every cancer type or other disease. This signature may provide information about disease status, aggressiveness, metastasis and response to therapy[1, 21,22]. Concerning the role of circulating miRNAs in cancer progression the later may be involved in cell-cell communication in order to deliver signals that regulate tissue microenvironment and promote carcinogenesis and spreading of cancer cells. miRNAs can be taken-up by nearby cells and act as oncogenes and oncosuppressors genes [23,25].

The first and of great significance miRNA that was linked with cancer was miRNA-21. Elevated levels of circulating miRNA-21 have been found in a variety of cancer types such as non-small cell lung (NSCL) and liver cancer, colorectal cancer[30], breast, ovarian and prostate cancer, oral, head and neck cancer, gastrointestinal cancer etc[1,25]. miRNA-21 has been describes as an oncogene because most of its target genes are tumor suppressors that down-regulates busting cell proliferation. Some of its targets are PDCD4 (main target) which is a tumor suppressor gene, multiple components of

TP53 and TGFB1. Other, miRNA-21 targets genes are associated with apoptosis, cell growth, migration and invasion such as BCL2, PTEN, RECK and others[1]. As it was mentioned, elevated levels of miRNA-21 are related with colorectal cancer. Specifically, serum and plasma miRNA-21 can be used for the early diagnosis for CRC, combined with the analysis of either other 3 miRNAs (miRNA-24, miRNA-320a and miRNA-423-5p) that are down-regulated or a panel of five miRNAs (let-7g, miRNA-31, miRNA-92a, miRNA-181b and miRNA-203) with 93% sensitivity and 91% specificity. Furthermore, high levels of serum miRNA can predict the CRC incidence with 90 % specificity and sensitivity[26,32].

1.2.2 Amplification-based methods for the detection of circulating miRNAs

A variety of methods have been performed for the amplification and detection of miRNAs, including NGS and PCR-based methods such as digital-PCR[34], RT-qPCR[35,36] and isothermal amplification methods such as LAMP, SDA, DSN, RCA (and its expansions) and others[35,37–40]. However, these methods have been tested and performed in specialized laboratories and not in clinical application.

NGS

As in the case of ctDNA, the advantage of NGS is the ability of multiplex expression analysis and identification and quantification of unknown miRNAs. Among the different NGS technologies, the "Sequencing- by-synthesis" technology by Illumina is widely used for the discovery of miRNA signatures or panels associated with diseases. In this approach, purified miRNAs are first ligated to adaptors at both ends, converted into complementary DNA (cDNA), amplified and analyzed.

Microarrays & Nanostring nCounter

In contrast to NGS, microarrays detect only known sequences. A microarray platform by Agilent (Agilent, Santa Clara, CA, USA) can measure in parallel all human miRNAs represented in the miRBase data base. Concerning the experimental procedure, purified miRNAs should be firstly tagged by fluorophores and then loaded in the platform followed by hours up to 2 days of incubation[36]. The sophisticated bioinformatics tools for the analysis and the need of a lot of time made these two methods inappropriate for routine clinical application. Another method for miRNA detection is the Nanostring nCounter platform. This is a barcoded hybridization-based, medium-throughput technology for measuring miRNA levels from low amounts of starting material without the need for reverse transcription or amplification[32].

PCR-based methods

The most common PCR-based method for miRNA detection and quantification is Revese Transcription (RT)-qPCR. There are two RT-qPCR approaches. In the first approach, the 3' end of miRNAs is extended with a poly(a) sequence via enzymatic treatment, followed by reverse transcription using a universal oligo(dT) primer. Then PCR with specific forward primer is performed and the product is detected using SYBR Green. During the second approach, a short single- stranded part of the stem-loop r prime was hybridized to the 3'of miRNAs and reverse transcribed with

reverse transcriptase. Then the RT products were quantified using conventional TaqMan PCR with miRNA-specific forward primer[35,36]. RT-qPCR is very slowly becoming applicable in clinical laboratory, mostly because the need of special instrument.

Isothermal methods

On the other hand, isothermal amplification methods, are conducted in one single stable temperature, need no cycling and not specific instrument so is more feasible to be applicable for easier and faster routine clinical diagnosis. Some of the isothermal amplification methods that have been used for miRNA detection are EXPAR (ExponentiaL Isothermal Amplification), LAMP (Loop-mediated Isothermal Amplification), DSN (Duplex Specific Nuclease), Rolling Circle Amplification (RCA) as well as molecular beacons.

During the EXPAR approach the target miRNA is triggering rounds of extension and cleavage its isothermal amplification after is hybridization on a specific designed template. Visualization of products occurred using SYBR green dye[40]. In a similar way, during DSN method the miRNA target hybridized with complementary Taqman probe, followed by selective cleavage of the RNA/DNA duplex by DSN the nuclease. The later, leads to the recycle of the miRNA and release the fluorescent part of the probe as well. However, in that case only one enzyme is used and no enzymatic amplification is performed. Finally, as concern LAMP, only Bst polymerase is used. miRNA hybridized on the 5' end of well designed template triggering polymerization by Bst polymerase and the appropriate sets of primers. In the end of each cycle Stem- Loop products are created which can bind SYBR Green I dye[40].

Table 2: Comparison of amplification-based methods for the detection of miRNAs

	Methods					
	PCR-based		Isothermal		Microaarrays[36]	NGS[36]
	RT-PCR[35,36]	digital-PCR[14,34]	L-RCA[40]	DSN[40]		
Advantages	Quantitative	Quantitative	Rapid Amplification	**Non-enzymetic amplification**	Partly Quantitatve	Quantitative
	Real-time		Sensitive			High-throughput
	Good sensitivity	Extreme sensitivity	Good Specificity	Use of only 1 enzyme	High-throughput	Detection of unknowm miRNAs
		High specificity	No need of special equipment			Discovery of miRNAs panels
	Good specificity		Flourescent detection		Good sensitivity	Sensitive/Accurate
Disadvantages	Special equipment needed/Requiers Cycling		Padlock-probe design	Uses Tqman Probes	High cost for rutine clinical practice	High cost
	Bioinformatics analysis		No absolute quantification			Time-consuming (up to days)
	Detects only known miRNAs					Special equipment needed
	Low-throughput					Requires expertise

1.3 Rolling Circle Amplification in Molecular Diagnostics

Apart from the above techniques, RCA is another isothermal DNA Amplification method that has been widely used for the detection of both DNA and RNA. RCA was the main method that used in this project, thus it will be extensively described.

Rolling Circle Amplification is an isothermal enzymatic DNA amplification method that developed in the mid-1990s. During RCA a short DNA or RNA primer initiate the amplification process using a circular DNA as template and a special DNA or RNA polymerase with strand displacement activity (Phi29, Bst, Vent exo-DNA polymerase and T7 RNA polymerase RNA). DNA or RNA polymerase replicates the circular template going around of it hundreds to thousands of times, resulting in the formation of a long single-stranded DNA (usually hundreds between hundreds of nanometers and microns in length) that contains tens to hundreds tandem repeats that are complementary to target sequence **(Figure 3A)**. Unlike PCR which requires thermal cycler, RCA can be conducted at constant temperature. The most suitable and widely used DNA polymerase for RCA reaction is phi29. This enzyme exhibits extreme processivity, strand displacement ability and has an optimal catalytic temperature at 30 ^{o}C. However, works well at room temperature (RT), too. A typical RCA reaction requires four components: phi29 DNA polymerase, a short DNA or RNA primer (which there are cases that serve as target, too), a circular DNA template typically (15–200 nt in length) and deoxynucleotide triphosphates (dNTPs). Due to the high processivity, fidelity and specificity of the reaction as well as the manipulation of the circular template and therefore the product, RCA has been explored extensively to develop sensitive detection methods for DNA, RNA, DNA methylation, single nucleotide polymorphism (SNP), small molecules and proteins. Moreover, there many researches demonstrating that RCA can be conducted directly in crude samples (cell extracts, serum)[41,42]. RCA seems to be suitable tool for the development of point-of-care detection methods.

RCA has been widely applied in nucleic acids analysis with the use of “padlock-probes”. Padlock probes are linear single stranded DNA probes of approximately 80-90 nt in length. The 5’- and 3’-end of padlock probes are designed to hybridize juxtaposed with the target nucleic acid such as genomic DNA or microRNA (miRNA). Then the two ends of the DNA probe are joined by a DNA liagse, creating DNA circles that serve as template for RCA reaction [21,43,44].

1.3.1 RCA Variants

Ligation-RCA (L-RCA) is one of RCA variants which is based in the procedure described above. During L-RCA **(Figure 3B)**, DNA ligases of high specificity could be used. Ligation and circularization of padlock probe (and subsequently RCA reaction) will be carried out only when there is accurate base pair complementation, enabling the detection/discrimination of point mutations (SNPs)[19,21]. Other RCA expansions are Multiprimed, Branched and Hyperbranched RCA (or RAM) **(Figure 3C)** and dumbbell-shaped probe RCA (D-RCA), Hairpin Probe (HP) -RCA and Toehold Mediated Strand Displacement RCA (TMSD)[35,40,43,44]. Multiprimed RCA can be performed by hybridization of more at least two primers in the same circular template initiating the amplification of multiple single-stranded RCA products. Single-stranded RCA products can be visualized by electrophoresis on agarose gel, incorporation of fluorescent dyes to RCA products via fluorophore-conjugated dNTP during RCA or atomic force microscopy[44]. On the other hand, BRCA and Hyper-BRCA methods are based in the addition of second primer (BRCA) or third primer (H-BRCA) that hybridized on the RCA product, creating the complementary RCA product, converted the single-stranded DNA to double-stranded. The dsDNA product can be visualized using SYBR Green I intercalating dye[43,44]. During

dumbbell or harpin-shaped probe RCA, a dumbbell-shaped instead of linear padlock probe is used as template for ligation and the DNA polymerase. Dumbbell probe has 3 domains, a target binding domain, a SYBR Green I binding domain and a loop binding domain. As concern the HP-RCA, as in previous case a well designed probe is used combined with SYBR Green I dye for visualization of

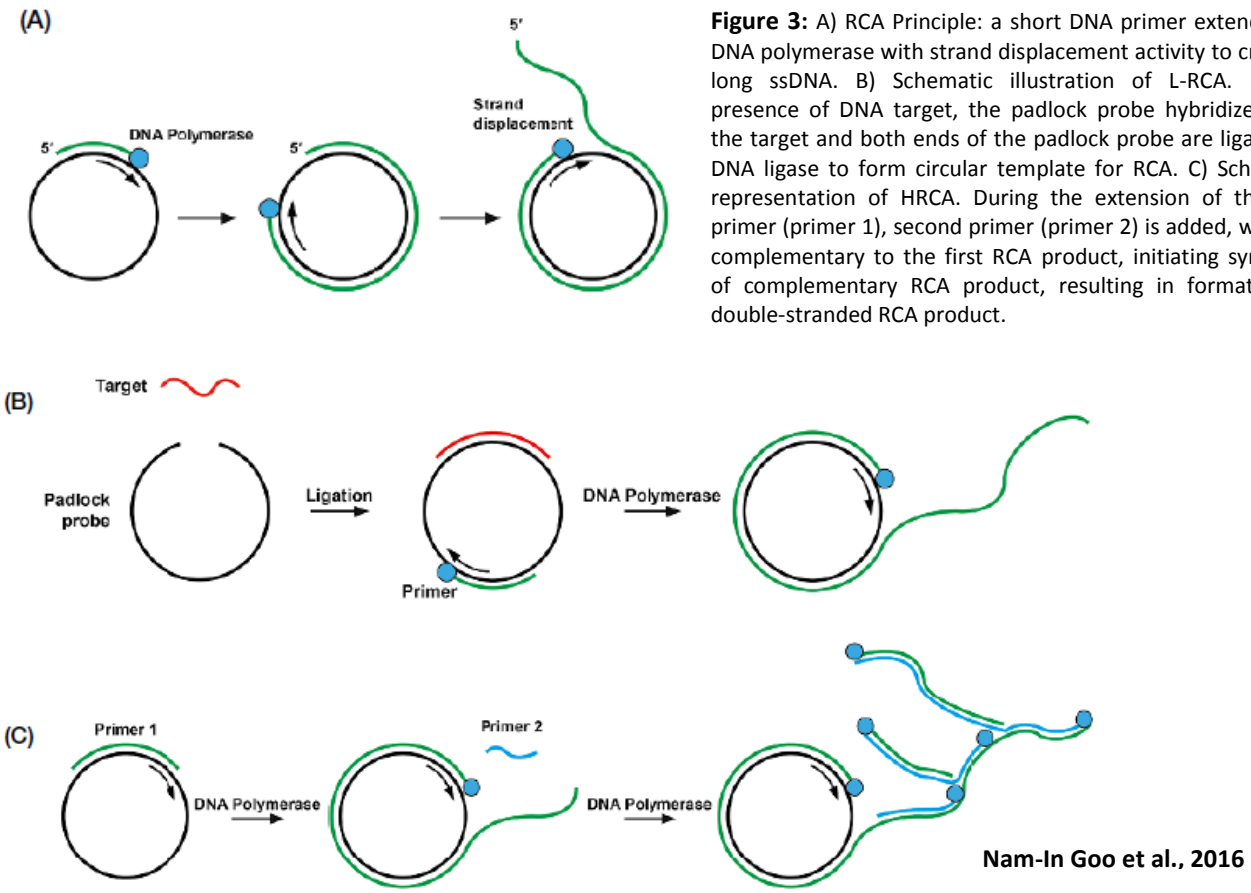

Figure 3: A) RCA Principle: a short DNA primer extended by DNA polymerase with strand displacement activity to create a long ssDNA. B) Schematic illustration of L-RCA. In the presence of DNA target, the padlock probe hybridizes with the target and both ends of the padlock probe are ligated by DNA ligase to form circular template for RCA. C) Schematic representation of HRCA. During the extension of the first primer (primer 1), second primer (primer 2) is added, which is complementary to the first RCA product, initiating synthesis of complementary RCA product, resulting in formation of double-stranded RCA product.

RCA product[40]. It is worth mentioning that in order to perform any type of RCA reaction, a ligation step for circularization should be conducted first, followed by RCA reaction. The two reactions are conducted separately in a sequential manner.

1.3.2 RCA for DNA/miRNAs detection

L-RCA is mostly used for the detection of SNPs or point mutations both in DNA or miRNAs[41,42]. Due to its high specificity and sensitivity RCA can induced signal amplification of target DNA sequences even when there is 1 copy of target in 100.000 copies of non-target DNAs[43]. On the other hand, all the methods described above have been extensively used for miRNA detection. miRNAs serve not only as a target, but also as primer. Using BRCA combined with the SYBR Green I dye 0.1 fM and 0.01 pg of target miRNA could be detected[38,43,46]. D-RCA and HP-RCA methods have been designed especially for miRNA detection. The LOD for both methods was 1 fM and 10 fM respectively.

1.4 Nanotechnology-based detection of nucleic acids

Advances in nanomaterials and nanotechnology contribute in the development of sensitive non-enzymatic amplification-based methods. For example, the bio-bar-code assay is characterized by extraordinary amplification and detection capability down to zM scale without enzymatic amplification, and has been applied for both miRNA and DNA detection. This technique utilizes two types of particles (a microparticle and a nonoparticle), each carrying an oligonucleotide partly complementary to the target so that can sandwich the target and accomplish sample purification, detection and amplification. The nanoparticle carries with it hundreds of oligonucleotides referred to as bar-codes. After sandwiched of target by the particles, a magnetic field and suitable treatment can be used to separate them from the sample solution, release the barcodes and detected using the scanometric method[40,47]. The target-triggered sandwich approach was also applied using a Liposome-QD(quantum dot)-probe and a capture-probe modified magnetic-beads (CP-MB). Again the LoD that was achieved was in aM levels[22]. Finally, Persano et al. at 2016 achieved label-free colorimetric detection of miRNA using magnetic microparticles and Au nanoparticles which carrying DNA probes complementary to the target miRNA, combined many rounds of strand extension, cleavage, and displacement which produces linker DNA triggering the sandwich formation. Detection of 1 fM initial template was achieved[48].

1.5 Biosensors in molecular diagnostics

As already stated there is an urgent demand for the development of sensitive, rapid, easy-to-use, cost-effective methods for the detection of circulating nucleic acids in biological fluids, suitable for clinical application. A major step was the development of novel, PCR-free, isothermal amplification strategies (for signal or DNA-target amplification). As already described nanomaterials and nanotechnology are great tools to contribute in the detection of biological targets with high sensitivity and efficiency, especially when combined with other techniques, such as biosensing methods. Incorporation of the amplification strategies with novel biosensors enables the development of easy-to-use diagnostic platforms or even portable point-of-care diagnostic systems removing the need of centralized laboratories and specialized personnel[33,45–47].

1.5.1 Introdunction to biosensors

A biosensor is an analytical device that uses a biological recognition system (bioreceptor) to target molecules or macromolecules (analytes). Biosensors use a physiochemical transducer to convert the signal from the bio-recognition system into a detectable signal. They consist of three main components: 1. the detector, which identifies the stimulus, 2. the transducer, which converts this stimulus (biorecognition event) to an output (measurable signal), and 3. the output system, which involves amplification and display of the output in an appropriate format. Biosensors are able to measure biological or chemical reactions by generating signals proportional to the concentration of an analyte in the reaction. However, a lot of information can be gained[52].

Biosensors can be classified into 3 main groups depending on the method of signal transduction: optical, electrochemical and acoustic (piezoelectric)[52–55]. In **optical biosensors**, detection is performed by exploiting the interaction of the optical field with a biorecognition element. They are further classified into labeled and labeled-free, where the detected signal can be either generated directly by the interaction of the analyte with the transducer or involves the use of a label and the optical signal is then generated by a colorimetric, fluorescent or luminescent method. Surface plasmon resonance (SPR), Ellipsometric and Surface-enhanced Raman scattering (SERS) are the most common optical label free biosensors[53]. **Electrochemical biosensors** detect the electrical signal that produce from the analyte "reaction" and is proportional to the analyte concentration. One of the key advantages of electrochemical biosensors is their relatively simplicity. Inexpensive electrodes and simple electronics can be easily combined to develop miniaturized easy-to-use portable systems[55].

Acoustic Biosensors

Acoustic biosensors operate by monitoring the change in the physical properties of an acoustic wave in response to the measurand. They are base in the piezoelectric phenomenon, which is displayed in certain crystals such as quartz where mechanical stress induces voltage generation and vice versa. Quartz crystal oscillates when an alternating voltage is applied producing acoustic waves. Acoustic wave sensors can be categorized according to the waves they generate depending on the cut of the quartz crystal into two main groups. Different cuts cause different piezoelectric deformation and subsequently acoustic waves that propagates into different directions. The two main "cuts" are AT and ST generating bulk and surface acoustic waves respsctively. Acoustic wave sensors are capable of detecting multiple physical parameters such as mass, viscoelasticity, pressure, temperature etc[54,56,57].

The well-established quartz crystal microbalance (QCM) is a BAW sensor comprising an AT-cut quartz crystal sandwiched between two circular electrodes, such as gold. Application of an alternating current (AC) voltage between the electrodes causes the crystal to deform in an oscillatory manner, preferentially operated in the fundamental thickness shear mode resonance or associated resonance overtones. This resonant frequency of oscillation of the crystal is sensitive to added mass at the crystal surface as described by Sauerbrey (1) allowing for quantitative measurements of changes at the crystal surface:

$$\Delta f = -\frac{2{f_0}^2 \Delta m}{A_{\text{piezo}}\left(u_q p_q\right)^{1/2}} \quad (1)$$

When molecules attached to the sensor's surface creates an elastic film and the frequency decreases proportional to the mass of the added molecules like it is described from the Equation (1)[54,56,58]. However, molecules are viscoelastic, which means that parts of them tend to resist distortion (viscocity) and parts of them tend to deform (elasticity) when a force is applied to them.

When such molecules are attach to the sensor surface, they form a “soft” film, and the Equation (1) does not fit.

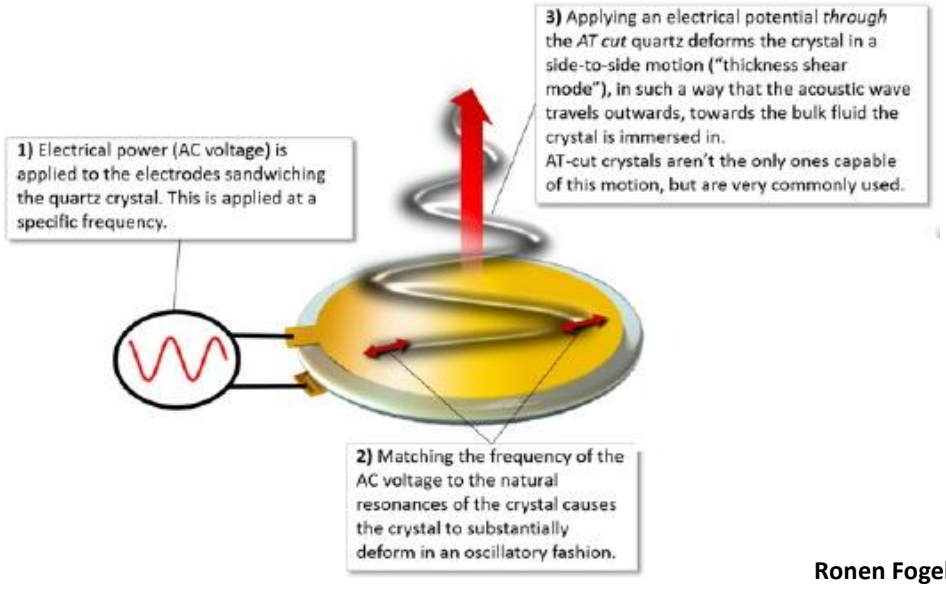

Ronen Fogel et al., 2016

Figure 4: Schematic representation of the general process for the generation of bulk acoustic acoustic wave on QCM.

QCM-D technology operates by monitoring the changes in the physical properties (frequency, **dissipation**) of the acoustic wave in response to a measurand presented at solid/liquid interface. Frequency changes (ΔF or ΔPh) of the acoustic wave depict changes of the elastic mass attached on the sensor surface. On the other hand, change in the acoustic energy dissipation depicts changes in viscosity during the loading and addition of samples. As molecules are viscoelastic, they also cause dissipation changes. Combining the changes in frequency and dissipation, information about the size, shape and intrinsic viscosity of surface-bound molecules (i.e. DNA structures, liposomes) can be obtained, too[54,58].

1.5.2 Biosensor-based detection of Circulating Nucleic Acids

A wide range of electrochemical, optical and acoustic techniques have already been integrated into biosensing analytical devices and/in order to applied in biomedical diagnosis and SNP detection. PNA probes immobilized on sensor surface of QCM[51], electrochemical and Surface enhance Raman spectroscopy (SERS) biosensor, have been widely applied in SNP detection, as they have a remarkable mismatch discrimination upon hybridization with complementary DNA. The detection limits for each case were 1 μg/mL, 62.41 amol/L, 3.4 pmol/L respectively. There is one electrochemical assay that is worth to be mentioned, which also utilize PNA probes; electrochemical clamp assay is a biosensing approach that has been applied directly in the serum of lung cancer patients for the detection of KRAS G13D point mutation in cfDNA using PNA probes. This assay is very fast and simple. Firstly, the heterogenous DNA/RNA sample is mixed with clamp sequences that will sequester via hybridization the wild-type sequence and all the KRAS mutants except from the mutant target of interest (KRAS G13D). Then the sample is applied to a PNA probe-

modified microsensor, and only the target mutant nucleic acids hybridize to the immobilized PNA probe, which is complementary to the target. The other mutants and wild-type nucleic acids are prevented from binding due to the clamps, and eventually are washed away. Electrochemical readout is following. The above assay achieved a detection limit of 10 fg/μL after 15 min of incubation for the hybridization with the PNA probe. However, during this assay it was detected both ctDNA and cfRNA[59].

Surface Ligation is another efficient method for SNP analysis that has been combined with SPR biosensor and leaky surface acoustic wave biosensor, achieving a detection limit of 1 pmol/L. Further technique for SNP detection combined the use of MutS missmatch binding protein with electrochemical biosensor: immobilized MutS on the electrode surface binds the SNP loci of heteroduplex DNA forming the electrical signal. The limit of detection that was achieved was 100 pmol/L[51]. However, based on the previous method QCM and SPR biosensing were applied, too. Finally, a label-free and sensitive method for SNP detection was developed by the combination of RCA and electrochemical biosensors. Using methylene blue as the electroactive indicator, the method enabled the detection of SNPs with a detection limit corresponding to 40 amol/L[20].

A wide range of miRNA biosensor-based assays have been developed including mainly electrochemical and optical approaches. Briefly, electrochemical label-free microRNA biosensor based on the cyclic enzymatic amplification method using T7[60] exonuclease or DSN[61] have been developed achieving a detection limit down to the fM level. Like in the case of MutS protein which binds mismatches in DNA duplexes, electrochemical sensors were developed using immobilized RNA capture probes and the p19 protein which binds on RNA duplexes. Since miRNA hybridizes on RNA probe, p19 binds with the hybrids of target miRNAs and their complementary sequences shielded the electrode surface, causing electrical signal[40,49]. LoD was from nM to aM levels. Other electrochemical label-free miRNA detection biosensor technologies was based on enzyme free quadratic SERS[62] signal amplification and carbon nanotube (CNT)[63] enhanced detection based on hairpin probe triggered RCA upon miRNA hybridization.

In order to achieve widespread use outside academic laboratories, nucleic acids detection assays must be cost-effective and easy to use. This is an important consideration when engineering signal amplification steps that require complicated liquid handling steps. Most of amplification assays and biosensors that have been developed have not yet been tested in clinically relevant samples such as blood, serum, plasma, saliva or urine. In most of the above cases that described, RNA and DNA isolation is required, regardless of which enzymatic-reaction based methods or nanotechnology-based methods used. Furthermore, most assays reported a limited SNP discrimination ratio (<10 fold), making them potentially unsuitable for detection of ctDNA. Despite that optical and electrochemical biosensing techniques have been widely developed, electrochemical and acoustic biosensors are more advantageous because are simpler, more cost-effective and label-free[22,40]. However, as concern the ctDNA and miRNA detection there are only few cases has been used acoustic biosensor.

1.6 Aim of the project

The overall aim of the project was the development of novel, easy, fast and reliable diagnostic methods for sensitive and efficient detection of a) circulating tumor DNA point mutations and b) circulating miRNAs, both treat cancer biomarkers, using RCA isothermal DNA amplification method combined with acoustic biosensor. As each nucleic acid target has its own characteristics (i.e. ctDNA is double stranded and more than 150 bp in length and miRNA is ssRNA and about 20nt), a suitable approach was designed to develop for each case.

As concern the detection of ctDNA point mutations, the aim was to develop a simple and fast (less than 2 hours) method which will detect and amplify ctDNA with sensitivity and high accuracy. The method will require very simple instrumentation, such as thermocycler, which is available any clinical laboratory and will be also suitable for integration in miniaturized portable devices (microfluidics, Lab on Chip), thus can be applicable in routine clinical diagnosis. As already stated, only few copies of ctDNA are presented in 5 mL of blood. Furthermore, ctDNA has very low quantities compare to "healtly" cell free DNA (1:10000). Thus, it is necessary the method to detect very low amount (even one copy) of the target with specificity. The addition of an optimal amplification step for ctDNA enhancement seems to be critical. RCA combined with a ligation step (L-RCA) has been proven suitable for sensitive SNP detection, achieving a detection limit at aM levels with good discrimination capability (mutant/WT 5000:1)[20]. By Introducing cycles of ligation-denaturation of padlock probe using a thermostable DNA ligase(AmpLigase), lower limit of detection at zM levels can be achieved as well. So enrichment through ligation followed by isothermal RCA amplification increase the number of DNA molecules eliminating the PCR-bias risk.

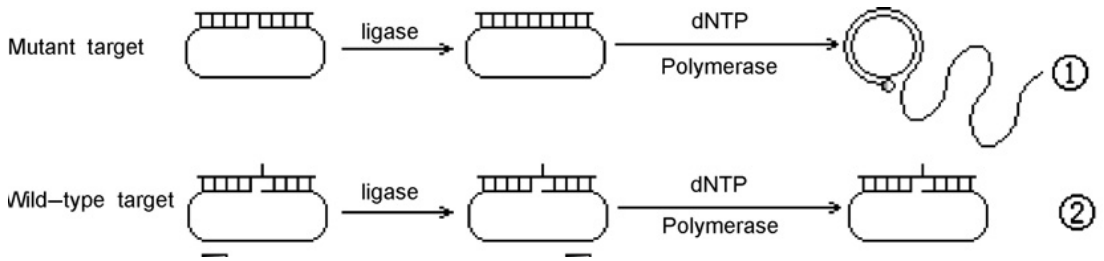

Figure 5: Amplification and enrichment of the mutant target via RCA
Circulization of padlock probe **only** occurs if there is accurate base pair complementation and only when the circle is complete, phi29 polymerase displaces the already existent product and carries on with the reaction going around of the target for many times

Amplified RCA products will then be detected using a commercially available acoustic based sensor, QCM-D device. There are only two studies that combined RCA with acoustic detection. Yao et al., 2013 achieved to detect 10^4 copies/mL of HBV genomic DNA with high specificity using a non-cycling ligation protocol and on-chip RCA-QCM. RCA was performed on the chip surface through capture probes which were immobilized on the gold electrode surface. First, the target strands act as a template for the circularization of the circular probe, and subsequently, a special primer triggers the isothermal amplification by phi29 DNA polymerase[64]. Previous study in the lab by Kordas et al., 2016 combined a Surface Acoustic Wave (SAW) device with RCA for rapid Salmonella

for targets amplification and detection. Various protocols were tested including off-chip and on-chip RCA. Finally, a limit of detection of 100 copies of Salmonella chemically synthesized DNA was achieved[65]. Both studies refer that the combination of RCA isothermal amplification with acoustic biosensor is very promising and has the potential to become a successful clinical application.

Take into account previous work of the lab[66] the method that was chosen for the bind of RCA product on to the sensor surface, was via PLL(25)-g-PEG(2) polymer. PLL-*g*-PEG is a random graft co-polymer with a poly(L-lysine) backbone and poly(ethylene glycol) side-chains. The PLL backbone is positively charged and interacts electrostatically with the negatively charged DNA, while the side-chains extend from the surface to form a densely packed polymeric brush. PEG side-chains consider as protein resistant. Due its nature of PLL-g-PEG, which is quite durable, no special manipulation is required. Direct loading and electrostatically absorption of non-purified RCA product to PLL(25)-g-PEG(2) coated gold sensors in order to be detected on QCM-D not only seems feasible, but also is a novel, easy and simple approach avoiding any complicated design and further steps. As a result, a novel method will be developed for the efficient detection of ctDNA point mutations via a two-step approach, which includes isothermal DNA amplification of high efficiency and specificity, followed by direct loading on QCM-D sensor.

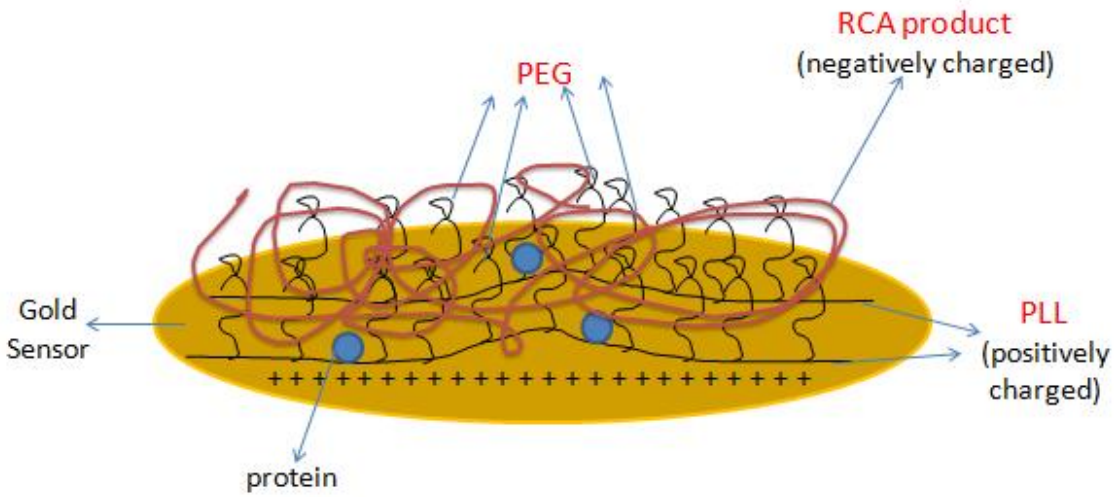

Figure 6: Adsorption of RCA product on PLL-*g*-PEG on gold coated QCM sensors.

Concerning the second case, altered levels of miRNAs and more specifically of miRNA-21, have been associated with multiple diseases, including cancer. miRNAs is presented in the circulation in quite higher levels compare with ctDNA, up to pM levels. Yanzhao Li et al., managed to discriminate patients with lung cancer from healthy people quantified the levels of miRNA-21 in blood via RT-PCR. Cancer patients had about three times higher levels of miRNA-21 (300 pM) in their circulation compare to healthy people (100 pM)[67]. As miRNAs can serve both as target for padlock circularization and as primer for RCA, RCA has been widely used for miRNA detection. However, multistep and complicated in design methods have been developed, required the use of different temperatures during the whole procedure and the need of cycler. Furthermore, in order to conducted RCA, ligation of padlock probe should be take place in a separate reaction prior RCA.

There is no published study, in which is referred the combination of ligation and amplification step into one. Take into account all the above as well as the fact that phi29 and more common ligases work well at RT and during the first part of the work it was managed the combination of ligation and amplification processes into one single step, here the aim of this project was the development of really novel, easy and efficient miRNA detection method, which will be constitute only from two steps and all the steps will be conducted at RT; 1. Ligation and amplification in one single step for the first time followed by 2. Acoustic detection using QCM biosensor. However the novelty of this case is that all the steps are conducted at RT (20 ^{o}C– 30 ^{o}C). No different temperatures and no thermal machine are required. About the detection on QCM-D device, two different approaches will be tested. Like in the previous case of ctDNA detection, the first approach that it will be tested is the binding of RCA product on gold sensor surface via PLL(25)-g-PEG(2). In the second approach binding of RCA product will be achieved via neutravidin protein. When RCA is conducted in presence of biotinylated-dUTP (b-dUTP), b-dUTPs will randomly incorporated in the RCA product, ensuring its binding on neutravidin. The same approach was used by Kordas et al., collecting notably data[65]. miRNA-21 is presented in high concentration not only in blood and its variants (serum, plasma) but also in saliva, where the 95 % constitutes from H_2O. Compatibility of the above method with application directly in crude samples (i.e. serum or saliva) would increase the chances for the development of a novel diagnostic platform or even better of a novel point-of-care system.

2. Materials & Methods

1. Acoustic Experiments

1.1 Quartz Crystal Microbalance experimental setup and crystal preparation

All the acoustic experiments described in this work were performed using QSense E4 instrument (Biolin Scientific) at the operating frequency of 5 MHz. QSense E4 is a QCM-D instrument consisting of 4-sensor chambers in a parallel configuration **(Figure 7)**. Prior to any acoustic experiment one or more (up to four) gold sensors with a fundamental frequency of 5 MHz and 14 mm total diameter from AW Sensors (AWS SNS 000042 A) were firstly rinsed by 70 % EtOH followed by nitrogen gas dry and then were subjected into high power plasma cleaning for 3 minutes using a Harrick plasma cleaner PDC-002. After cleaning, gold crystals were immediately transferred to their chambers. All the experiments were carried out at 25 ^{o}C, in a continuous flow of buffer solution at the constant flow rate of 50 µL/min using a peristaltic pump. After the measurement was stopped, the chambers including the gold sensors were cleaned with 2% Helmanex and ddH_2O and reused. The real-time data were collected and further analyzed using QTools and OriginPro 8. Resonance frequency and Energy dissipation changes were measured at the 7th overtone.

1.2 Real-Time Acoustic Detection of RCA on PLL(25)-g-PEG(2) coated sensors

Acoustic measurements were performed under the continuous flow of Tris buffer (10 mM, pH=7.5) (Sigma). Briefly, gold sensors were firstly equilibrated with Tris buffer. Then, 30µg of PLL(25)-g-PEG(2) (diluted in Tris buffer up to 300 µL (0,1% w/v) were independently injected to each gold sensor followed by buffer rinsing and the addition of Single-step or Two-Step RCA positive or negative reactions in the PLL-g-PEG coated sensors. Again buffer rinsing took place. RCA positive and negative reactions were also diluted in the running buffer up to 200 µL, prior to the addition. In every case, after the washing step the real-time signal is supposed to reach a plateau. The absorption of the polymer on the gold electrode was verified by typically detecting $\Delta F \approx -235$ Hz, $\Delta D \approx +3 * 10^{-6}$ at the 35 MHz overtone and 0.013 for the acoustic ratio.

1.3 Real-Time Acoustic Detection of RCA on Neutravidin coated sensors

PBS (2.7 mM KCl, 8.1 mM Na2HPO4, 1.76 mM KH2PO4, 137 mM NaCl, pH 7.4) (Sigma) with or without MgCl2 or Tris (20 mM pH=7.5) (Sigma) or MES (45 mM, pH 5.5) (Sigma) buffer was pumped over the gold-coated surface of the sensor in a continuous flow-throw manner. Again, gold sensors were firstly equilibrated with the running buffer. Then, 200 ng/µL neutravidin (Invitrogen) was added independently on the gold surface of each sensor, followed by buffer rinsing until the real-time signal reach a plateau. After washing, addition of Single-step RCA positive or negative reactions in the neutravidin coated sensors took place followed by buffer rinsing. All the samples were diluted in the running buffer up to 200 µL.

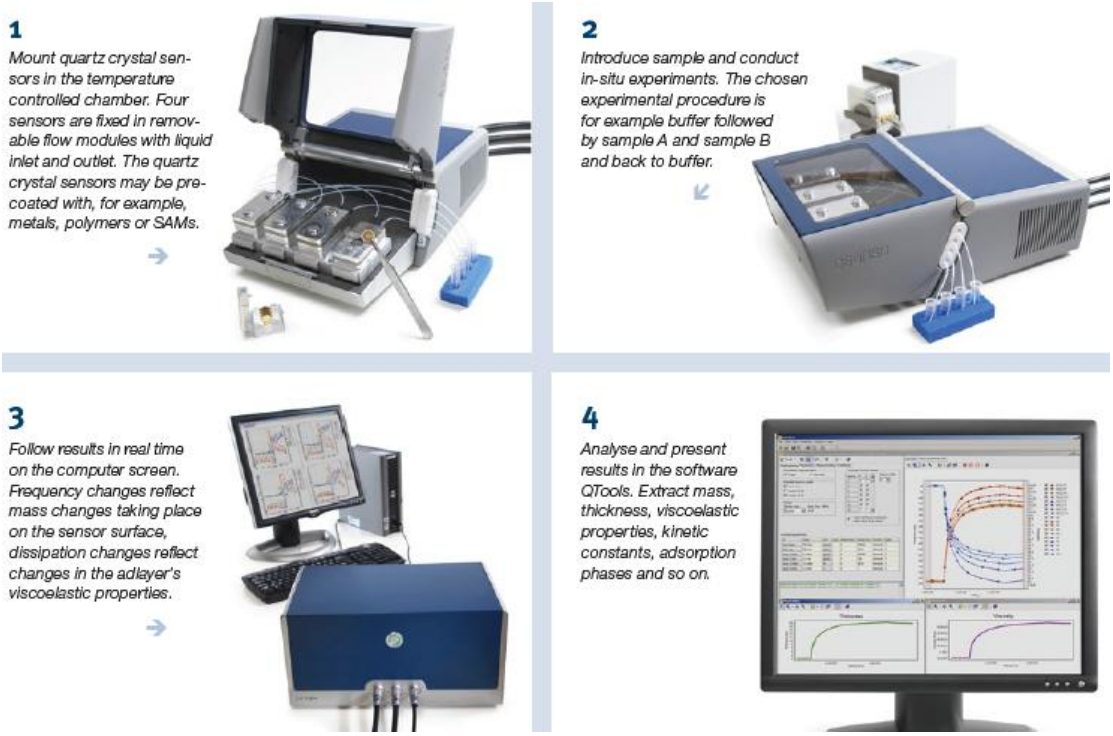

Figure 7: Representation of QCM-D set up.

2. Design and List of Oligonucleotides

Oligonucleotides, including those mimicking the Circulating Nucleic Acids (ctDNA carrying the KRAS G12D mutation and miRNA-21) as well as primers and probes, were synthesized by Metabion International AG, unless otherwise stated. Two different single-stranded DNA oligonucleotides (85nt and 21nt) corresponding to KRAS gene target which carry a mutation at codon 12 and another two single-stranded DNA oligos (22nt) mimicking the WT sequence of miRNA-21-5p or carrying a mutation in the middle of its sequence were synthesized. These targets can be used first of all, as a template for the circularization of padlock probes and in some cases as primer in order Rolling Circle Amplification (RCA) to be performed. Concerning the padlock probe design, each probe consisted of an oligonucleotide of 70-80 bases in length. Both 5' and 3' ends of the probes bore 11-20 nt that hybridize to the complementary sequence of target, immediately 5' and 3' of the mismatch respectively, with the 3' terminal base to vary in the case of KRAS-target. Two padlock probes have been synthesized for the KRAS G12D target (which carries the mutation), one fully complementary to the target and the other with a mismatch in the 3' end which corresponds to the WT sequence of 12 codon. As concern the miRNA-21 DNA target only one padlock probe were synthesized, with accurate base pair complementation to the WT sequence. One set or primers was used for the PCR amplification of 85nt KRAS G12D in order to be converted to double stranded DNA and one or more primers were designed and used in each case for RCA. All sequences are presented in **Table 1**.

Table 1: Names and sequences of DNA targets, padlock probes and primers

DNA Oligo	Sequence (5'->3')
Target Sequences	

KRAS G12D 85 nt (DestTarget1)	TTAGCTGTATCGTCAAGGCACTCTTGCCTACGCCA**TC**AGCTCCAACTAC CACAAGTTTATATTCAGTCATTTTCAGCAGGCCTTA
KRAS G12D 21 nt oligo (PMT)	GTT GGA GCT **GA**T GGC GTA GGC
miRNA-21-5p^{WT} (T21WT)	TAGCTTATCA**GA**CTGATGTTGA
miRNA-21-5p^{MT} (T21MT)	TAGCTTATCA**GC**CTGATGTTGA
Padlock Probes	
KRAS Pdlk WT (PadWT)	**CAGCTCCAACTACCACAAGT** TTATTAAGTCAGTATCGTCCGGAT CCTAGCAT AG **GCACTCTTGCCTACGCCAC**
KRAS Pdlk MT (PadMT)	**CAGCTCCAACTACCACA** AGTTTATTAAGTCAGTATCGT CCG GATCCT AGCATTAG **GCACTCTTGCCTACGCCAT**
PdlK21 WT (Pdlk21)	**CTGATAAGCTA** ACT GCA TCG TGG AGA TTC TCA GCC AGA CC AAC CCA TCA GGA TAG ATC GCG CTA AGC **TCAACATCAGT**
PCR Primers	
KRAS 85nt Fw (Set1fw)	TTAGCTGTATCGTCAAGGCACTCTTGCCTA
KRAS 85nt Rv (Set1rv)	TAAGGCCTGGTGAAAATGACTGAATATAAA
RCA Primers	
KRAS-PL (PdlkP1) (Minotech)	TACTGACTTAATAAACTTGTGG
KRAS-PR (PdlKP2) (Minotech)	GTGCCTAATGCTAGGACCGG
KRAS-PM (BamProbe)	ATG CTA GGA TCC GGA CGA TAC TGA
P21-left (P21-1)	GGC TGA GAA TCT CCA CGA TG
P21-right (P21-2)	GCG CGA TCT ATC CTG ATG GG
P21-middle (P21-3)	TCC TGA TGG GTT GG TCT GGC

3. PCR amplification of KRAS G12D 85 nt

Single-stranded KRAS G12D 85 nt target was converted to double-stranded DNA after PCR amplification using the KAPA2G Fast HotStart ReadyMix PCR Kit from KAPABIOSYSTEMS. 3ng of single-stranded DNA was mixed 5 µL of 2X KAPA2G Fast HotStart ReadyMix and 10 pmol of each KRAS 85 nt Fw and Rv primers in a final volume of 10 µL. After an initial denaturation at 95 ^{o}C for 5min, 35 cycles followed of 10 sec denaturation at 95 ^{o}C, 10 sec annealing at 60 ^{o}C, 10 sec extension at 72 ^{o}C and a final extension step of 1 min at 72 ^{o}C. PCR product was extracted using the Nucleospin PCR Clean-Up protocol of the *NucleoSpin Gel and PCR Clean-up Kit* by *Macherey-Nagel.*

4. Preparation of Padlock Probes

In order the padlock probes to be circulated and act as a template for phi29 DNA polymerase for the conduction of Rolling Circle Amplification, phosphorylation of their ends has to be performed prior to ligation. The 5' termini of 300 pmol linear padlock probe were phosphorylated by T4 Polynucleotide Kinase (3' phosphatase minus) (New England Biolabs). The reaction has a final volume of 50 µL and contains 10 units of T4 Polynucleotide Kinase (3' phosphatase minus), 1x T4 Polynucleotide Kinase Reaction Buffer, 1mM ATP and 0.1 µg/µL BSA. The reaction was incubated at

37 °C for 30 min, followed by heat inactivation of T4 PNK at 65 °C for 20 min. All reagents were purchased from New England Biolabs.

5. Rolling Circle Amplification (RCA)

Phosphorylated padlock probes can be ligated into circles (circularization) in a target-based manner, providing the template for the specific hybridization of one or more primers and the conduction of RCA by phi29 DNA polymerase. Usually target-based padlock ligation and RCA are conducted in two separately steps (two-step RCA Reaction), however, the combination of these two steps into one can be achieved as well (single-step RCA Reaction).

For the detection of KRAS G12D point mutation two chemically synthesized KRAS DNA targets were designed and used. The DNA targets were 21 nt and 85 nt in length and they will be referred as KRAS G12D 85 nt and KRAS G12D 21 nt Oligo respectively. Both targets carry the G12D point mutation in about the middle of the sequence. Moreover, two padlock probes complementary to either the mutant (KRAS Pdlk MT) or the wild type (KRAS Pdlk WT) G12D targets were designed, too. The latter was used as control. Theoretically, ligation of the linear padlock **only** occurs if there is accurate base pair complementation and **only** when the circle is complete, phi29 polymerase displaces the already existent product and carries on with the reaction going around of the target for many times. To investigate the detection of miRNA-21-5p, it was designed and used a chemically synthesized single stranded DNA oligo, instead of RNA, with the miRNA sequence (miRNA-21-5p^{WT}), as well as a second DNA oligo with the miRNA-21-5p sequence however carrying a point mutation (mismatch) exactly in the middle of its sequence (miRNA-21-5p^{MT}). Furthermore, one single padlock probe (Pdlk 21 WT) with the 11 bases of its 5’ and 3’ ends fully complementary to the miRNA WT sequence was used.

Ligation constitutes the most critical step concerning the specificity of the method. During the experiments it was tested the ligation performance of three different enzymes; T7 DNA Ligase, AmpLigase Thermostable DNA Ligase and T4 DNA Ligase. T7 DNA Ligase is an ATP-dependent Ligase from bacteriophage T7 that catalyzes the formation of a phosphodiester bond between adjacent 5´ phosphate and 3´ hydroxyl groups in duplex DNA structures. T7 DNA Ligase works better at 25°C and can be heat inactivated at 65°C. AmpLigase thermostable DNA Ligase derived from a thermophilic bacterium and catalyzes the NAD-dependent ligation of adjacent 3´-hydroxylated and 5´-phosphorylated termini in duplex DNA structures **only** when there is **perfect complementation.** Furthermore, AmplLigase is extremely thermostable and completely active at high temperatures (half-life is 48 hours at 65°C and more than 1 hour at 95°C) so that can be subjected into rounds of denaturation and ligation producing many minicircles (circularized padlock probes). T4 DNA Ligase is ATP dependent and catalyzes the formation of a phosphodiester bond between juxtaposed 5' phosphate and 3' hydroxyl termini in duplex DNA or RNA. Moreover, this enzyme can repair single stranded nicks in duplex DNA and some DNA/RNA hybrids making it appropriate for miRNA detection.

<u>5.1 Two-Step RCA Reactions</u>

Two-step RCA reactions have been conducted for the detection of double stranded KRAS G12D 85nt target and single stranded KRAS G12D 21 nt oligo, using two different ligation enzymes, AmpLigase - Thermostable DNA Ligase (Epicentre) and T7 DNA Ligase (New England BioLabs). All reagents were purchased from New England Biolabs (NEB), unless otherwise stated.

5.1.1 Ligation using AmpLigase

2.5 units of AmpLigase were mixed with varying concentrations of ds KRAS G12D 85 nt target and 0.5 pmol of phosphorylated KRAS Pdlk MT or WT padlock probes. The reaction has a final volume of 15 µL and contains 1x AmpLigase buffer (Epicentre) and 0.04 µg/µL BSA. After an initial incubation of the reaction at 94 ^{o}C for 5 min to denaturate target DNA, 40 cycles of incubation at 92 ^{o}C for 5 sec and 62,5 ^{o}C for 10 sec were performed for circularization of padlock probe. performed either by using phosphorylated KRAS Pdlk WT padlock or without addition of DNA target.

5.1.2 Ligation using T7 DNA Ligase

Ds (85 nt) or ss (21 nt) KRAS G12D target was mixed with 3000 units of T7 DNA Ligase, 0,5 - 2 pmol phosphorylated KRAS Pdlk MT or WT padlock probes, 1mM ATP and 0.1 µg/µL BSA in 1x NEB buffer 4 in a final volume of 20 µL. The mixture was incubated at 25 ^{o}C for 30 min followed by enzyme inactivation at 65 ^{o}C for 10 min. In the case of ds DNA target it is required the addition of an extra step, where denaturation of the target in presence of padlock probe takes place. Control reactions were performed either by using phosphorylated KRAS Pdlk WT padlock or without any addition of DNA target.

RCA Reaction

The whole ligation mixture of AmpLigase was used directly for RCA. However, in the case of T7 DNA Ligase 5-10 µL of ligation mixture were used. In both cases, the latter was mixed with 5 units of phi29 DNA polymerase in 1x phi29 DNA polymerase Reaction buffer, 200 µM dNTP mix, 0.1 µg/µL BSA and 10 pmol of KRAS-PM primer in a 25 µL final reaction volume. RCA reaction was then incubated at Room Temperature (RT) or at 30 ^{o}C for 30 to 120 minutes followed by enzyme inactivation at 65 ^{o}C for 10 min. Then, RCA products were analyzed in 1% agarose gel stained with GelRed (Biotium) along with 100 ng of λ DNA-BstEII DNA marker. Gels were visualized after 45 – 60 min of electrophoresis at 130 V–140 V using a UV station.

5.2 Single-step RCA Reactions

Single-step RCA reactions have been conducted for the detection of single stranded KRAS G12D 21 nt oligo, using the ligation enzymes AmpLigase (Epicentre) and T7 DNA Ligase (New England Biolabs), as well as for the detection of miRNA-21-5p^{WT} and miRNA-21-5p^{MT} using T4 DNA Ligase (New England BioLabs). All reagents were purchased from New England Biolabs (NEB), unless otherwise stated.

5.2.1 Combined RCA & Ligation using AmpLigase

Different concentrations of KRAS G12D 21 nt were mixed with 0.5 pmol phosphorylated KRAS Pdlk MT or WT padlock probes in the presence of 2.5 units AmpLigase and 5 units of phi29 DNA

polymerase. The reaction has a final volume of 25 μL and contains 0.4x AmpLigase Assay buffer, 1x phi29 DNA polymerase Reaction buffer, 200 μM dNTP mix, 0,1 μg/μL BSA and 10 pmol of KRAS-PM primer. The mixture was incubated at Room Temperature (RT) for 10 – 30 min, followed by enzyme inactivation at 65 ^{o}C for 10 min and electrophoresis for 45 -60 min in 1% agarose gel stained with GelRed (Biotium) along with 100 ng of λ DNA-BstEII DNA marker. Control reactions were performed using phosphorylated KRAS Pdlk WT padlock.

5.2.2 Combined RCA & Ligation using T7 DNA Ligase

KRAS G12D 21 nt DNA target were mixed with 0.5 pmol phosphorylated KRAS Pdlk MT or WT padlock probes in the presence of 3000 and 5 units of T7 DNA Ligase and phi29 DNA polymerase respectively. 1mM ATP, 200 μM dNTP mix, 0.1 μg/μL BSA and 10 pmol of KRAS-PM and/or KRAS-PL / KRAS-PR primers were added, too. The reactions were conducted in 1x phi29 Reaction buffer and 0.8x NEB buffer 4 in a final concentration of 25 μL. Mixtures were incubated at 25 ^{o}C for 10-30 min followed by enzyme inactivation at 65 ^{o}C for 10 min. RCA products were analyzed in 1% agarose gel stained with GelRed (Biotium) along with 100 ng of λ DNA-BstEII DNA marker. Gels were visualized after 45 – 60 min of electrophoresis at 130 V–140 V using a UV station. Control reactions were performed either by using phosphorylated KRAS Pdlk WT padlock or without any addition of DNA target.

5.2.3 Combined RCA & Ligation using T4 DNA Ligase

440 units and of T4 DNA Ligase (New England Biolabs) were mixed with various concentrations of miRNA-21-5p$^{WT/MT}$ and 2 pmol of phosphorylated Pdlk 21 WT, as well as 10 units of phi29 DNA Polymerase. The reaction has a final volume of 25 μL and contains 0.8x NEB buffer 4, 1x phi29 DNA Polymerase Reaction buffer, 0.1 μg/μL BSA, 1 mM ATP and 10 pmol of P21-middle primer and/or 10 pmol of each P21-Left / P21-Right primer or without any addition of primer. The reactions have been conducted in presence of 400 μM dNTP mix (dATP, dCTP, dTTP, dGTP - NEB) which in some cases they were containing 400 nM to 40 μM of biotin-dUTP (Metabion) (1/100 - 1/10 compare to dTTP in respect) with the corresponding reduction in dTTP. Reactions were incubated at RT for 30 - 210 minutes followed by cold inactivation (transfer at -20 ^{o}C) until their subsequent use. The latter could be either electrophoresis at 130 V–140 V for 45 – 60 min in 1% agarose gel stained with GelRed (Biotium) along with 100 ng of λ DNA-BstEII DNA marker or dilution in the appropriate buffer up to 200 μL and loading on PLL(25)-g-PEG(2) or neutravidin coated gold sensors. No heat inactivation was performed. Control reactions were performed without addition of DNA target

Table 2 summarizes all the Rolling Circle Amplification protocols.

Table 2.1: Two-step RCA protocols

	Two-step RCA			
	AmpLigase (Epicentre)		T7 DNA Ligase (NEB)	
Reagents	***Ligation***	***RCA***	***Ligation***	***RCA***
DNA target/template (Metabion)	ds KRAS G12D 85 nt	15 µL Ligation mix	Ds (85 nt)/ss (21 nt) KRAS G12D	5 - 10 µL Ligation mix
Padlock probe (1µM) (Metabion)	0.5µL KRAS Pdlk WT/MT	-	0.5 - 2 µL KRAS Pdlk WT/MT	-
Primer (10 µM) (Metabion)	-	1 µL KRAS-PM	-	1 µL KRAS-PM
dNTP mix (10 mM of each	-	0.5 µL	-	-
dATP, dCTP, dGTP, 9.9 mM of dTTP (NEB) & 0.1 mM b-dUTP (Metabion))	-	-	-	-
dNTP mix (10 mM of dATP, dCTP, dGTP, 9 mM of dTTP (NEB)	-	-	-	-
b-dUTP (1 mM) (Metabion)	-	-	-	-
ATP (10 mM) (NEB)	-	-	2.5 µL	-
BSA 1µg/µL (stock 20 mg/mL) (NEB)	1.5 µL	-	2.5 µL	1 µL
BSA 1µg/µL (stock 10 mg/mL) (NEB)	-	1 µL	-	2.5 µL
phi29 DNA polymerase Buffer 10x (NEB)	-	2.5 µL	-	-
NEB buffer 4 10x	-	-	2 µL	-
AmpLigase Assay Buffer 10x (Epicentre)	1.5 µL	-	-	-
AmpLigase (5 U/µL) (Epicentre)	0.5 µL	-	-	-
T7 DNA Ligase (NEB)	-	-	0.5 µL	-
T4 DNA Ligase (NEB)	-	-	-	-
phi29 DNA polymerase (10 U/µL) (NEB)	-	0.5 µL	-	0.5 µL
ddH2O	up to 15 µL	up to 25 µL	up to 20 µL	up to 25 µL

Table 2.2: Single-step RCA protocols

	Single-Step RCA				
	AmpLigase (Epicentre)	**T7 DNA Ligase (NEB)**	**T4 DNA ligase (NEB)**	**T4 DNA ligase (NEB) -**	**T4 DNA ligase (NEB) -**
Reagents	***Combined Ligation & RCA***				
DNA target/template (Metabion)	KRAS G12D 21 nt	KRAS G12D 21 nt	miRNA-21-5p$^{WT/MT}$		
Padlock probe (1µM) (Metabion)	0.5 µL KRAS Pdlk WT/MT	0.5 µL KRAS Pdlk WT/MT	2 µL Pdlk21 WT		
Primer (10 µM) (Metabion)	1 µL	1 µL KRAS-PM/PL /PR	1 µL P21-3/1/2 or w/o	1 µL P21-3 or w/o	
dNTP mix (10 mM of each dNTP) (NEB)	0.5 µL	0.5 µL	1 µL	-	-
dNTP mix (10 mM of dATP, dCTP, dGTP, 9.9 mM of dTTP (NEB) & 0.1 mM b-dUTP (Metabion))	-	-	-	1 µL	-
dNTP mix (10 mM of dATP, dCTP, dGTP, 9 mM of dTTP (NEB)	-	-		-	1 µL
b-dUTP (1 mM) (Metabion)	-	-	-	-	1 µL
ATP (10 mM) (NEB)	-	2.5 µL	2.5 µL		
BSA 1µg/µL (stock 20 mg/mL) (NEB)	-	-	-		
BSA 1µg/µL (stock 10 mg/mL) (NEB)	2.5 µL	2.5 µL	2.5 µL		
phi29 DNA polymerase Buffer 10x (NEB)	2.5 µL	2.5 µL	2.5 µL		
NEB buffer 4 10x	-	2 µL	2 µL		
AmpLigase Assay Buffer 10x (Epicentre)	1 µL	-	-		
AmpLigase (5 U/µL) (Epicentre)	0.5 µL	-	-		
T7 DNA Ligase (NEB)	-	0.5 µL	-		
T4 DNA Ligase (NEB)	-	-	1 µL		
phi29 DNA polymerase (10 U/µL) (NEB)	0.5 µL	0.5 µL	1 µL		
ddH2O	up to 25 µL	up to 25 µL	up to 25 µL		

3. Results

As already stated the aim of this project was the detection of circulating nucleic acids associated with cancer. Specifically, ctDNA and its KRAS G12D point mutation, as well as circulating miRNA-21, both associated to colorectal and lung cancer was used as the main targets to be detected. In both cases, the method is based on two main steps: a) The amplification and enrichment of target by RCA followed by b) the detection of the amplified product using the QCM biosensor. As mentioned before, the first step includes two different processes. Firstly, a ligation process where linear padlock probes are ligated into single-stranded circular DNA in a target-based manner. Then, one or more specific primers are hybridized to the circular template and phi29 DNA polymerase can elongate the product, followed by **amplification** by phi29 DNA polymerase.

3.1 Detection of KRAS G12D point mutation

3.1.1Detection of KRAS G12D 21 nt oligo

The first set of experiments included Specificity and Time Assays for both T7 DNA Ligase and AmpLigase using as template the KRAS G12D 21 nt Oligo. Since not only phi29 DNA polymerase and T7 DNA work well at RT, but also AmpLigase maintains a good catalytic activity it was initially tried for both ligases the combination of the ligation and amplification processes into one single reaction. In these experiments, 10 pmol of the target which carried the point mutation were mixed with 0.5 pmol of either the KRAS Pdlk MT (fully complementary to the target) or KRAS Pdlk WT (contains a mismatch at 3' end) padlock probe and with the two enzymes (polymerase and ligase). The reactions were incubated for 10', 20' and 30' at RT (20 to 25 ^{o}C) and the RCA products were analyzed on 1 % agarose gel **(Figure 8)**. Both ligases showed increased specificity. However, a small amount of un-specific product has been created in the case of T7 DNA Ligase after 30 min of incubation. The same reactions were conducted changing the incubation time to 2' and 5'. As it seems in **Figure 9**, 2' of incubation are enough to produce visualized RCA products.

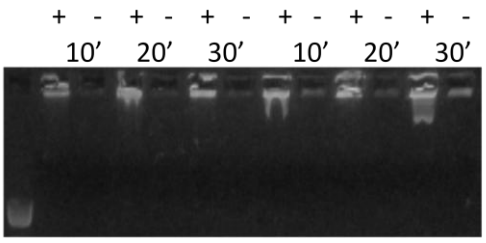

Figure 8: RCA specificity results with Ampligase and T7 DNA ligase using KRAS G12D 21nt oligo and 0.5 pmol of MT or WT padlock probe.
Left to right: Ladder/ Lanes 2-7: AmpLigase / Lanes 8-13: T7 DNA Ligase. Both Ligases creates specific products after 20 min of incubation and only in the case of T7 Lgase a small amount of un-specific product has been created after 30 min of incubation. WT padlock was used as negative control.

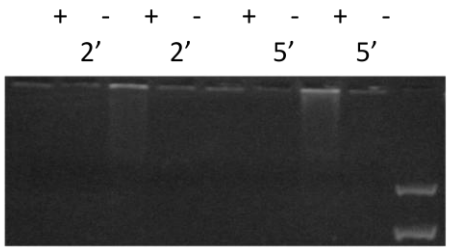

Figure 9: Single-step RCA (positive vs negative) in 2-5 min using KRAS G12D 21nt oligo and 0.5 pmol of MT or WT padlock probe.
Lanes 1-2 & 5-6: AmpLigase / Lanes 3-4 & 7-8: T7 Ligase.
Visualized RCA products can be created after 2 - 5 min of incubation using T7 DNA ligase.

Since 25 ^{o}C is the optimal temperature for T7 DNA liagase and the latter cannot be subjected into cysles of denaturation and ligation the next step was to identify the limit of detection (LOD) for T7 DNA Ligase at RT and/or in single step reaction. So, both single-step and two-step reactions that contain 0.5 pmol of KRAS Pdlk MT padlock probe and 0.1 pmol, 0.1 fmol of KRAS G12D 21nt oligo or no target (control) were prepared and incubated at RT for 1 to 2 hours concerning the amplification step. As concern, the two-step reaction, before the amplification step have preceded 30' of ligation at RT. Again the amplified products were analyzed on 1 % agarose gel. In both cases, 0.1 pmol create visualized product. However it is worth mentioning that in the case of single step reactions there was non-specific amplification. The non-specific products are probably due to self-ligation of the padlock probe and are avoided by separating the ligation from the amplification step, like in two-step reactions **(Figure 10)** or by conducted the incubation for no more than 30' in one step reaction. In the latter case, the limit of detection for the T7 Ligase was the 1 fmol of initial target using 0.5 pmol of padlock probe **(Figure 11)**.

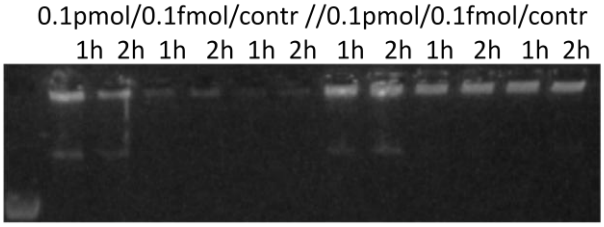

Figure 10: RCA LOD & specificity results for T7 DNA Ligase in 2-step (Lanes 2-7) and 1-step (8-13) reaction using KRAS G12D 21nt oligo and 0.5 pmol of MT padlock probe.
2 step Reaction: 30' Ligation followed by heat inactivation & 1h – 2h incubation for RCA .1 step Reation: Combined Ligation & RCA into one reaction & 1h - 2h incubation for RCA. In both cases, 0.1 pmol created visualized products with increased specificity. However, during single-step reactions there was non-specific amplification in control and probably for 0.1 fmol target. Control reactions were w/o addition of target DNA.

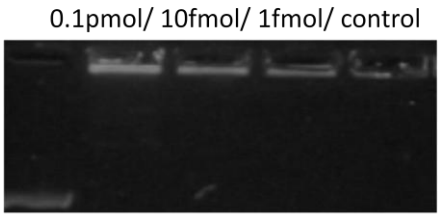

Figure 11: RCA LOD results for T7 DNA Liagase after 30' single step reaction, using KRAS G12D 21nt oligo and 0.5 pmol of MT padlock probe.
1 fmol of initial DNA target It was detected with increased specificity. Control reactions were w/o addition of target DNA.

In order to further decrease the LOD of a 30' single step reaction with T7 DNA Ligase, it was investigated the effect of using two primers which were hybridized left (KRAS-PL) and right (KRAS-PR) of the padlock probe, instead of the one primer which binds in the middle (KRAS-PM) of the padlock's sequence. Theoretically, by using two primers -or three including the 21 nt oligo target-, multiple copies of RCA product is generating from a single circle. However, the best production of RCA was managed using the KRAS-PM primer **(Figure 12 & 13)**.

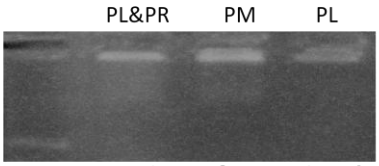

Figure 12: Comparison of one-primed single-step RCA with multiple-primed.
10 fmol of KRAS G12D 21nt oligo and 0.5 pmol of MT padlock probe were mixed with one or more primers. Lane2: 2-primed (KRAS-PL & KRAS-PR) RCA product (primers hybridized near the ends of the padlock probe), Lane 3 & 4: single primed RCA product (primer hybridized on the middle -KRAS-PM- or near the 5' end -KRAS-PL- of padlock sequence). More RCA product was obtained using one middle primer.

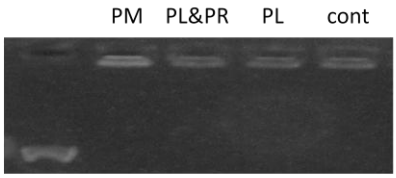

Figure 13: Comparison of one-primed single-step RCA with multiple-primed.
1 fmol of KRAS G12D 21nt oligo and 0.5 pmol of MT padlock probe were mixed with one or more primers. Lane 2: single-primed RCA product (KRAS-PM primer hybridized on the middle of padlock's sequence), Lane 3 & 4: 2- (KRAS-PL & KRAS-PR) and 1- (KKRAS-PL) primed RCA product respectively (primers hybridized near the ends of the padlock probe or at 5' end), Lane 5: negative control. 1 fmol of the target was detected only when the KRAS-PM primer was used.

3.1.2 Detection of KRAS G12D 85 nt

A second set of experiments was conducted using KRAS G12D 85 nt DNA target. First step was the conversion of single-stranded KRAS G12D 85 nt target (carrying the G12D mutation) to double-stranded DNA by PCR amplification followed by purification using the Nucleospin PCR purification kit. Then, LOD assays again for both AmpLigase and T7 DNA ligase were performed.

The use of dsDNA fragment as template for the RCA reaction required the addition of one more step where DNA will be heat denaturated for approximately 5 min at 95°C. Then, the denaturated target was mixed with 0.5 pmol of either the MT (fully complementary to the target) or the WT (contains a mismatch at 3' end) padlock probe. Using T7 DNA ligase it was successfully detected specific RCA products from 100 pg of dsDNA template (100 pg of ds target correspond to 10^6 copies) within 120 min of incubation at RT during 2-step reaction (3-step including the denaturation process) **(Figure 14)**. However, it was managed to detect 10 pg of ds target during single-step reaction (2-steps in total including the denaturation step) as well **(Figure 15)**.

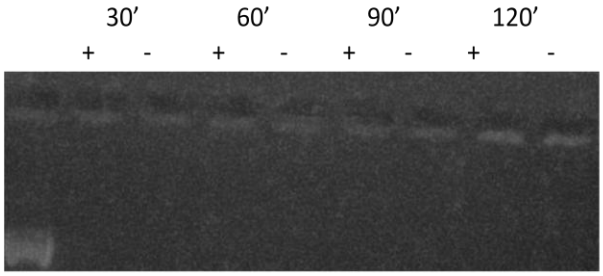

Figure 14: RCA with T7 DNA ligase from 100 pg (10^6 copies) of ds KRAS G12D 85 nt template & 0.5 pmol of MT or WT padlock probe in 2 step reaction.
100 pg of the target were successfully detected after 5' denaturation, 30' of ligation & 120 min for RCA at RT. WT padlock was used as negative control.

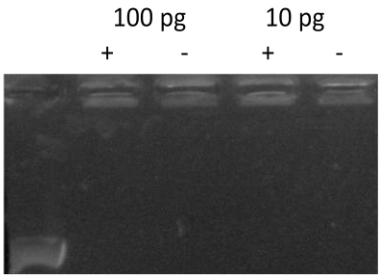

Figure 15: Detection of 10 pg of ds KRAS G12D 85 nt template using T7 DNA Ligase in single step reaction.
100 pg (Lane 2) & 10 pg (Lane 4) of target were mixed with 0.5 pmol of either MT or WT padlock probe. Both were successfully detected after 30 min of combined ligase and RCA at RT. WT padlock was used as negative control.

In the case of AmpLigase only two-step RCA reactions were conducted for the detection of ds KRAS G12D DNA target. Performing a cycling protocol of denaturation and ligation with 0.5 pmol of padlock probe enhanced the creation of minicircles and subsequently the template for RCA. As a result, an extremely low limit of detection of approximately 10 copies was achieved within 30 min of RCA reaction **(Figure 16)**. The protocol duration in total was about 30 min for cycling (denaturation and ligation) and another 30 min of incubation for RCA at 30 ^{o}C. In all cases, RCA products were analyzed on 1 % agarose gel.

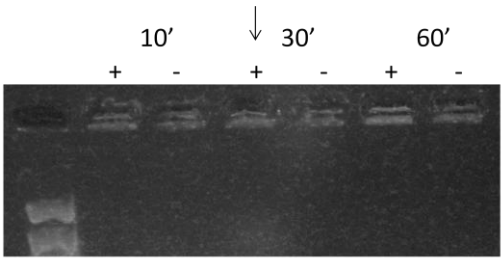

Figure 16: RCA with Ampligase from 10 copies ds KRAS G12D 85 nt starting template.
10 copies of initial target were mixed with 0.5 pmol MT or WT padlock probe followed by incubation for 30' in a cycling protocol and other 10', 30' & 60' for RCA at 30 ^{o}C. 30' of RCA was enough to result visualized RCA products.

3.1.3 Detection of KRAS G12D on QCM biosensor

Since it has been investigated the ligation performance of the two ligases and a very good LOD has been achieved using 2-step AmpLigase reaction and gel analysis electrophoresis next step was to tested the detection of RCA product using an acoustic biosensor. For these experiments the commercially available Quartz Crystal Microbalance (QCM-D) setup was used where acoustic measurements were carried out at 35 MHz. As already stated, an acoustic experiment is conducted in a continuous flow-through manner involving steps of sample loading and buffer washing in an alternate way. Briefly, in this case substrate-coated gold sensors interact, absorb or bind the RCA product. The presence of the sample at the sensor's surface affects the propagation characteristics of the acoustic wave, which can be monitored as changes in frequency (ΔF) and energy dissipation (ΔD). Frequency changes correspond on the amount of adsorbed mass and dissipation on the viscoelastic properties of the bound molecules (Acoustic detection of DNA conformation in genetic assays combined with PCR).

Interesting results have been obtained from previous work of the lab about PLL(25)-*g*-PEG(2)/(5) polymer and how the latter interact electrostatically with dsDNA and binds it to the sensor surface. Better results have been obtain for the PLL(25 kDa) grafted with PEG(2 kDa) (PLL(25)-*g*-PEG(2)). PLL-*g*-PEG is a random graft co-polymer with a poly(L-lysine) backbone and poly(ethylene glycol) side-chains. The PLL backbone is positively charged and interacts electrostatically with the negatively charged DNA, while the side-chains extend from the surface to form a densely packed polymeric brush. PEG side-chains consider as protein resistant.

The electrostatically adsorption of non-purified RCA product to PLL(25)-g-PEG(2) coated gold sensors in order to be detected on QCM-D seemed to be not only feasible, but also the easier and simpler way. So, 2-step AmpLigase RCA reactions were prepared using 1 pmol of ss KRAS G12D 21

nt oligo with 0.5 pmol of either the MT (positive) or WT padlock (control MM) padlock probe as well as without initial template (negative). The reactions were incubated about 30 min in the cycling protocol and 60 min for RCA at 30 ^{o}C. Then, acoustic experiments were performed using E4-Qsense instrumenet. In all cases, there was a continuous flow at 50 µL/min of Tris 10 mM. Gold sensors were firstly coated with PLL-*g*-PEG and then, 17 µL of the 25 µL of each reaction were loaded on them. The absorption of the polymer on the gold electrode was verified by typically detecting ΔF ≈ -235 Hz, ΔD ≈ +3 * 10^{-6} at the 35 MHz overtone and 0.013 concerning the acoustic ratio **(Figure 17A)**.

Since no pre-existing data were available for changes in frequency and dissipation concerning the addition of un-purified RCA product on PLL-g-PEG, both frequency and dissipation changes as well as the acoustic ratio (ΔD/ΔF) were calculated and compared. In every case, differences in frequency and dissipation were measured when the washing-off phase was complete, and the signal has reached a plateau (plateau(after)-plateau(before), *after & before: the addition of sample). The most clear results were collected concerning the changes in dissipation where positive was at least 2.5 times higher than the controls. In that case positive was easily distinguished from both negative and mismatch controls **(Figures 17 & 18)**. The average values were 3.3 ± 0.67 *10^{-6}, 1.17 ± 0.43 *10^{-6} and 1.52 ± 0.23 *10^{-6}, respectively. Similar, but not so clear results were obtained comparing

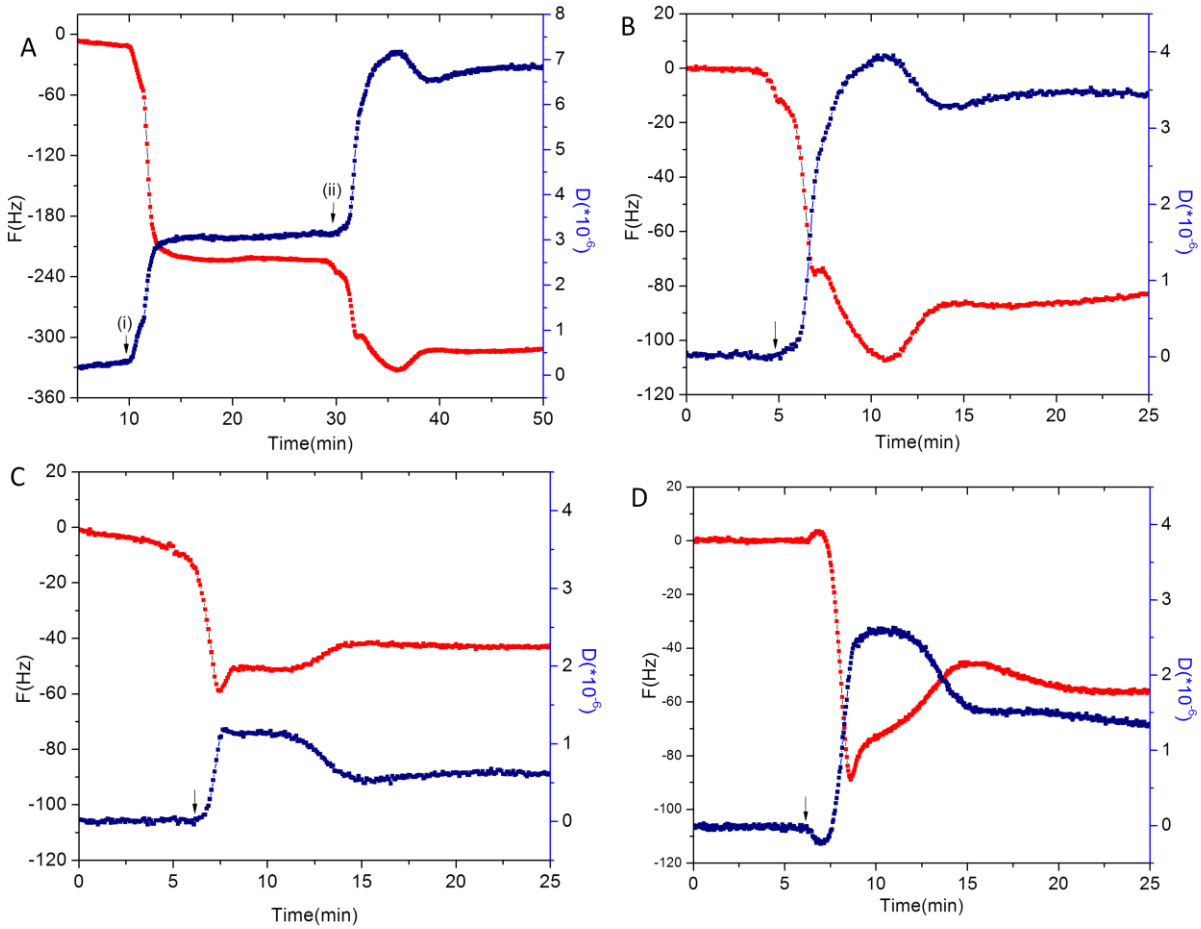

Figure 17: Schematic overview of acoustic detection of RCA from 1 pmol ss KRAS G12D 21 nt template after 2- step reaction with AmpLigase on PLL(25)-g-PEG(2): Graphs represent the real time acoustic curves. The red and the blue lines depict changes in the frequency and energy dissipation of the acoustic signal respectively. The black arrows indicate the time points where the sample touches the sensing area. **A)** The first step (i) corresponds to the adsorption of PLL-g-PEG on the gold surface of the acoustic device followed by buffer rinsing. The following step (ii) corresponds to the subsequent addition of positive RCA sample. **B), C), D)** only the second step of sample addition is shown, skipping the polymer absorption. Graphs correspond to positive, negative and mismatch control respectively.

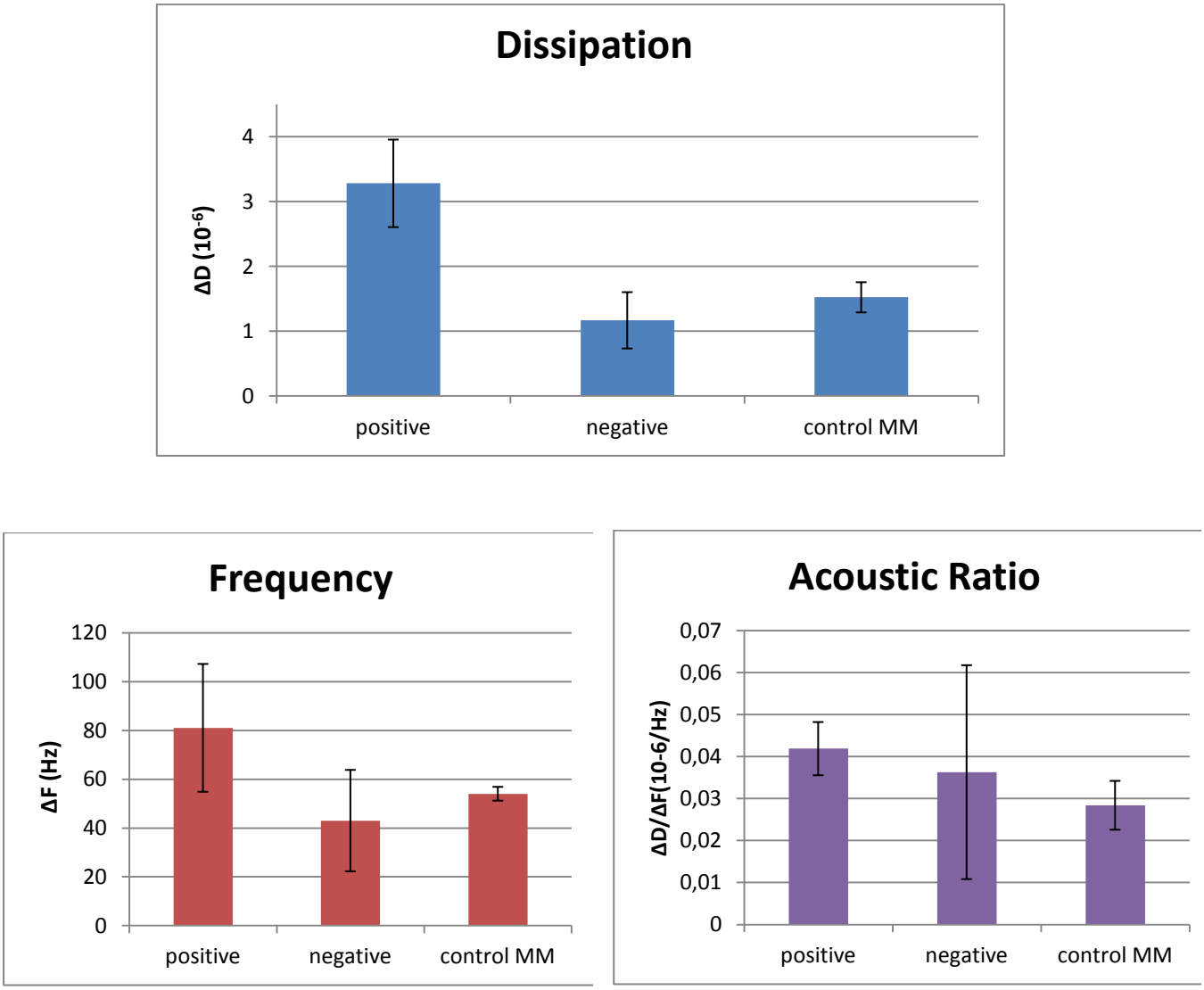

Figure 18: Comparison of Dissipation & Frequency changes as well as the acoustic ratio between positive reaction, negative (w/o template) and mismatch control (control MM).
2-step RCA reactions with AmpLigase were conducted for 1 pmol ss KRAS G12D 21 nt template followed by loading on PLL(25)-g-PEG(2). In every case, acoustic measurements were performed when the washing-off phase was complete, and the signal has reached a plateau (plateau(after)-plateau(before), *after & before the addition of sample). (N = 4 for positive & negative, N = 2 for control MM). *N = Number of experiments)

changes in frequency. The average values were 81 ± 26.2 Hz, 43 ± 20.8 Hz, 54 ±2.8 Hz for positive, negative and mismatch control in respect. However, the values for acoustic ratio were significantly varying for negative control, and as a result did not distinguish neither from positive nor from mismatch control.

3.2 Detection of miRNA-21

3.2.1 Investigating the ligation performance of T4 DNA Ligase

In a first set of experiments it was investigated the ligation performance of T4 DNA ligase as concern the specificity and its LOD in a single step reaction at RT, without followed by enzyme inactivation by heat (for more details see Materials & Methods: *Combined RCA & Ligation using T4 DNA Ligase).*1 pmol of either the WT or the MT miRNA-21, as well as no miRNA-21 were mixed with 0.5 pmol of padlock probe in a 30' single step reaction at RT. As already mentioned, the aim in these set of experiments was everything to be conducted at RT, without the need of incubating at different temperatures or using special machines. So, no enzyme inactivation by heat were performed after the end of the reaction. Instead, the reactions were immediately transferred on ice or were loaded and analyzed in 1 % agarose gel. As T4 DNA Ligase can repair nicks in DNA/RNA hybrids, it was not really expected to have increased specificity in the case of mismatch. However, no un-specific product was detected when there was not any addition of template, which means that there is not any auto-ligation of padlock probe **(Figure 19)**. About the LOD, the clinical relevant limit of miRNA-21 is about 100 to 300 pM (270 pM in cancer patients) in the blood (or serum) of healthy and cancer patients, respectively[67]. So, 1 to 10 fmol (40 to 400 pM) of miRNA-21^{WT} were mixed with 2 pmol of padlock probe and one or w/o the addition of primer (miRNA-21 can act as a primer, too). The reactions were single step, incubated for 120 min and 60 min respectively and were not heat inactivated. RCA products were analyzed on 1 % agarose gel. Both 1 and 10 fmol were detected and amplified. However, a larger amount of amplified product was obtained without the addition of primer **(Figure 20)**. This can be due to the different rate that phi29 and T4 DNA liagse act on DNA. In other words, probably phi29 DNA polymerase which has a polymerization rate about 50 nt/sec, displaces T4 DNA ligase before ligation of padlock probe is completed.

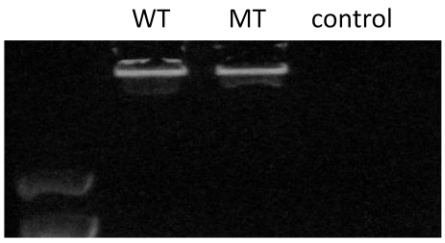

Figure 19: T4 DNA Ligase Specificity results.
Lanes 2-3: Ligation of padlock probe were performed almost with the same efficiency in both miRNA-21 WT & MT (carrying a mismatch on the ligation site). Lane 4: No un-specific profuct were detected when there was not initial template.

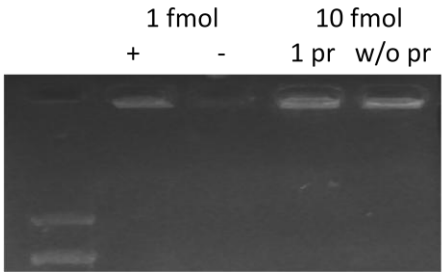

Figure 20: Detection of 400 - 40 pM of miRNA-21
Lane 2-3: 1 fmol or no template & Lane 4: 10 fmol of miRNA-21 were mixed with 2 pmol of padlock probe in single step reaction for 120 & 60 min respectively, at RT. In both cases visualized RCA products were created. Lane 5: More RCA product was created without addition of primer.

3.2.2 Detection of miRNA-21 using a QCM-D set up

Next step was to investigate the detection of RCA product using the QCM-D setup. All acoustic measurements were carried at 35 MHz. Many factors were tested in order to achieve the best result concerning the LOD on QCM biosensor and the repeatability and reliability of the method. Some of them were a) the substrate for the binding of RCA product b) the buffer and the c) ionic strength, as well as the incubation time of the Single-step RCA reaction at RT **(Table 3)**. However, all the acoustic experiments can be divided in two main categories according to the immobilization method of RCA product on the sensor surface. These two main methods were either by PLL(25)-g-PEG or by the neutravidin-biotin interaction.

Table 3: Summary of the different factors and combinations that were tested during acoustic experiments.

Substrate	Buffer	pH	b-dUTP compare to dTTP	Incubation Time (min)
PLL(25)-*g*-PEG(2)	Tris 10 mM	7.5	-	30
Neutravidin	150 mM PBS - 10 mM MgCl2	7.4	1/100	30
				60
			1/10	60
	Tris 20 mM	7.5	1/10	60 to 210
	MES	5.5	1/10	60

3.2.2 A) Acoustic detection of RCA on PLL-*g*-PEG coated gold sensors

Single-step reactions with 1 pmol and 10 fmol miRNA-21 as initial target were prepared and incubated for 30' at RT. After, the incubation was over, reactions were immediately transferred on ice, until their loading on the sensor. Again, acoustic experiments were performed using E4-Qsense instrumenet. All the experiments were conducted in a continuous flow of buffer Tris 10 mM. In every case, the whole RCA reaction (25 µL) was loaded on PLL-g-PEG coated gold sensors. As it was previously described differences in frequency and dissipation were measured when the washing-off phase was complete, and the signal has reached a plateau (plateau(after)-plateau(before), *after & before: the addition of sample). At first glance, only the reactions of 1 pmol initial template could be distinguished from the negative control, and only as concern the changes in dissipation. The average values were 9 ± 1.86 $*10^{-6}$, 3.4 ± 1.3 $*10^{-6}$ and 5.5 ± 1.2 $*10^{-6}$ for 1 pmol, 10 fmol and negative control respectively **(Figure 21)**. However, at least three remarks worth mentioning. Firstly, in these set of experiments much higher dissipation and frequency changes were obtained (both the values of the average value and standard deviation) compare to these of the acoustic detection of KRAS G12D RCA on PLL-g-PEG. Secondly, negative control has very big values and thirdly, the values of standard deviation were significant high, especially in the case of negative control, affecting the repeatability and reliability of the above results.

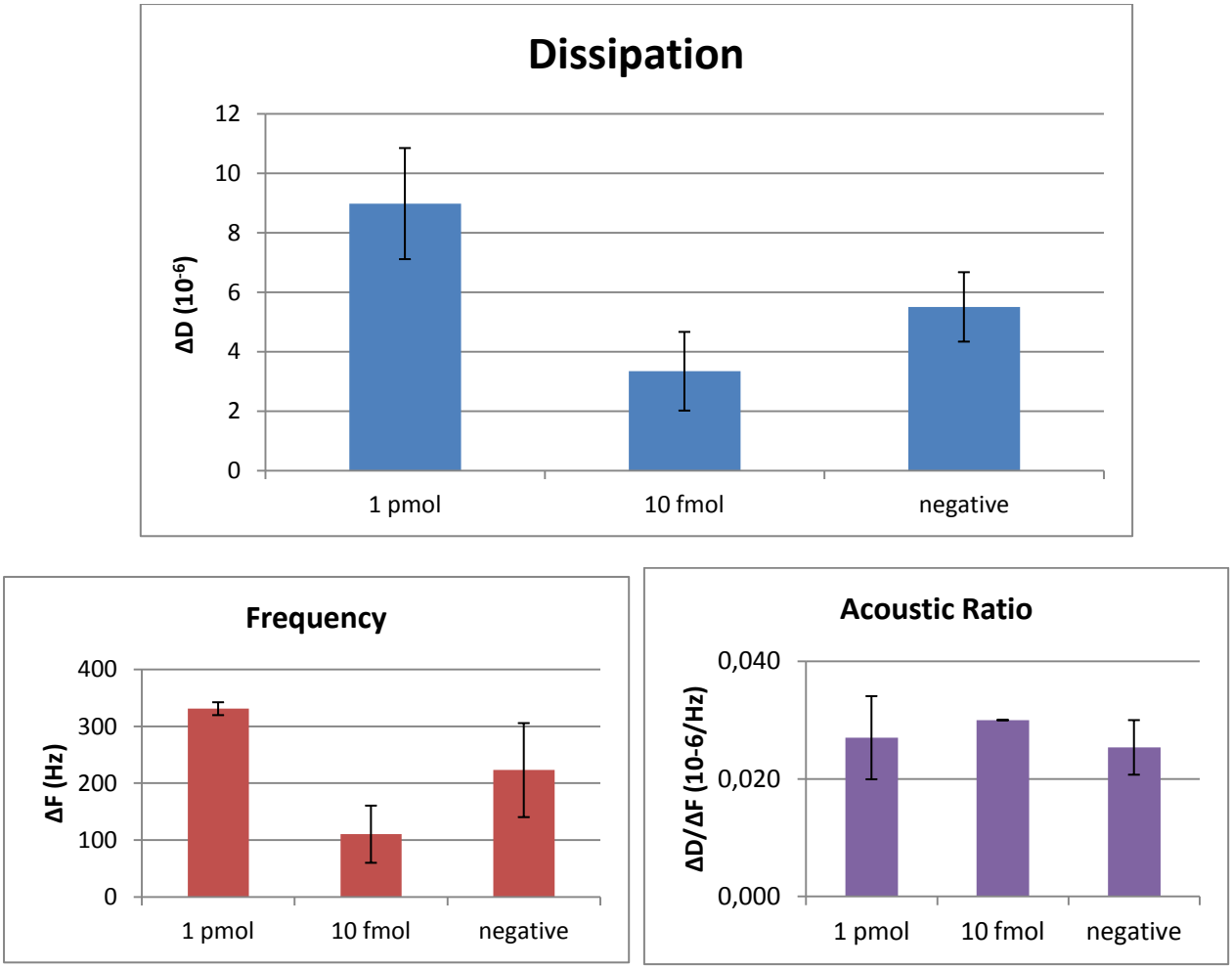

Figure 21: Comparison of Dissipation & Frequency changes as well as the acoustic ratio between reactions of 1 pmol - 10 fmol initial template and negative control (w/o template).
30' single-step RCA reactions with T4 DNA ligase were conducted for 1 pmol & 10 fmol of miRNA-21 DNA target followed by loading on PLL(25)-g-PEG(2). In every case, acoustic measurements were performed when the washing-off phase was complete, and the signal has reached a plateau (plateau(after)-plateau(before), *after & before the addition of sample). (N = 2 for 1 pmol & 10 fmol N = 4 for negative. *N = Number of experiments)

It was suspected that the so high and so different ΔD and ΔF values were due to the effect of reaction's buffers, the enzymes and the large amount of BSA (2.5 μg) contained in the reaction as well as because of the un-specific absorption of all these on PLL-*g*-PEG. Not only DNA, but also BSA is negatively charged at pH 7.5 and possibly the enzymes, too. Moreover, in the case of of T4-RCA reaction the whole reaction was loaded in each case and not only the 17 μL of the 25 μL. So, in order to investigate how the different substances/materials of the reaction mix affect the acoustic signal a number of reaction mixes (like control) were prepared and loaded on PLL-g-PEG coated sensors, following the same procedure as in a usual experiment (Materials & Methods: Real - Time Acoustic Detection of RCA on PLL(25)-g-PEG(2) coated sensors). The reaction mixes were (see the table below):

Reaction mix	Materials
Nucleic Acids (NA)	Padlock probe, dNTPs, ATP, primer
Buffers + Enzymes + BSA	phi29 Reaction buffer, NEB buffer 4, phi29 DNa pol., T4 DNA Ligase, BSA
Buffers + BSA + NA	phi29 Reaction buffer, NEB buffer 4, BSA, Padlock probe, dNTPs, ATP, primer
Buffers + Enzymes + NA	phi29 Reaction buffer, NEB buffer 4, phi29 DNa pol., T4 DNA Ligase, Padlock probe, dNTPs, ATP, primer

As it seems in **Figure 22,** indeed the high changes in dissipation and frequency is mainly due to BSA, a bit less due to the enzymes and buffers, while NA were almost undetectable.

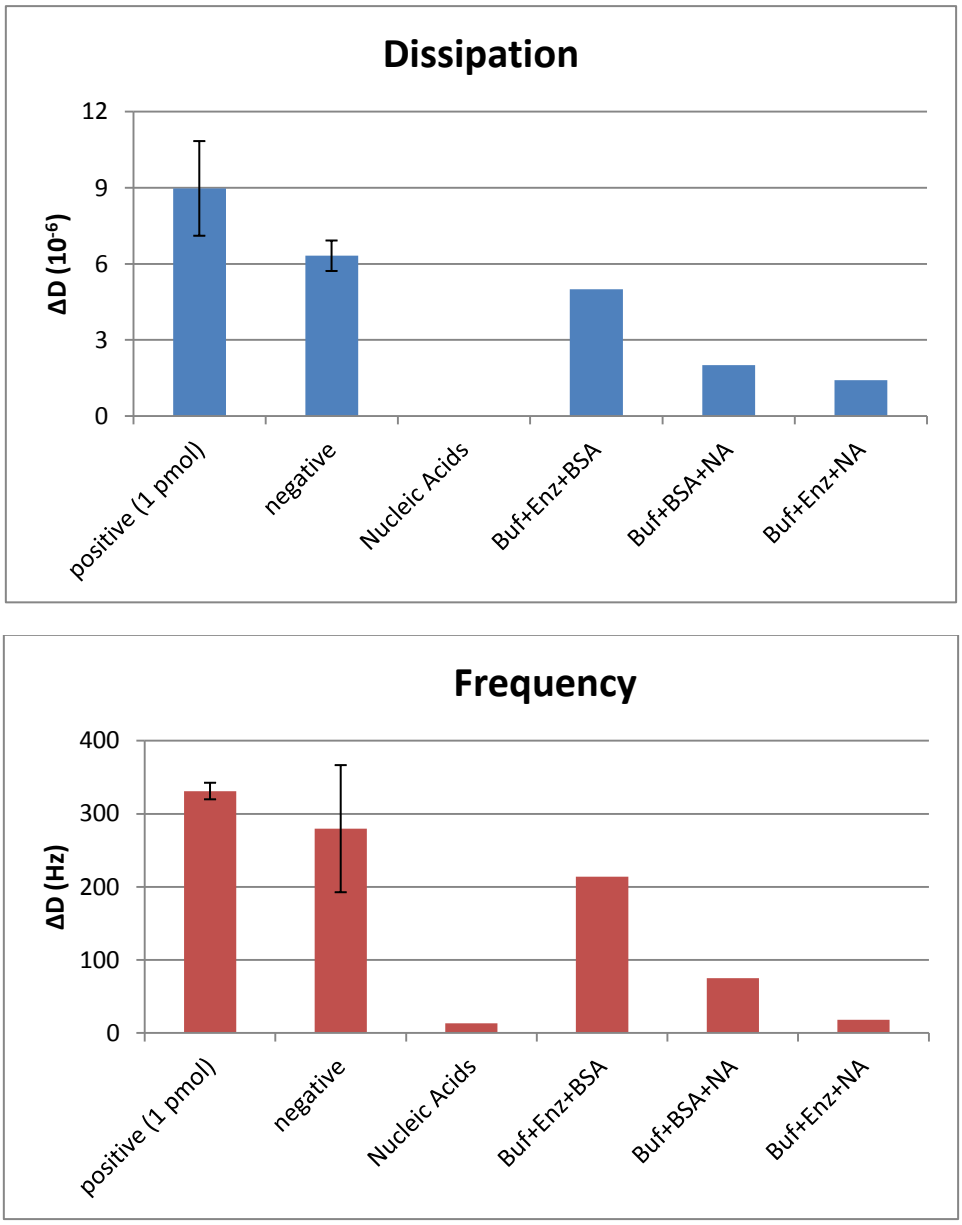

Figure 22: Effect of buffers, enzymes, BSA & NA in dissipation and frequency changes: Reaction mixes of different constitution concerning the addition of buffers, BSA, enzymes and NA were loaded on PLL(25)-*g*-PEG(2) following the same procedure as in a usual experiment.

Thinking the results of the KRAS G12D RCA on PLL-g-PEG, first of all 15 of 25 µL of the final reaction was submitted in cycling up to 65 ^{o}C - 95 ^{o}C (this constitutes the first step of 2-step reaction with AmpLigase). This means that both the ligase and the largest amount of BSA were fully denatured. Secondly, during the second step of the two-step RCA, phi29 was heat inactivated by incubation at 65 ^{o}C. Thirdly, exactly the half amount of both Ligase and phi29 were added in those reactions compare with the T4 - single step reaction of the case here.

Finally, it was tested to reduce the addition of BSA/reaction from 25 ng to 10 ng combined with the use of another BSA purchased from different company (Sigma-Ardich). Since single-step RCA reaction was compatible with the above changes and worked equally well, firstly same amount of BSA from sigma, diluted in Tris buffer, was added on PLL-g-PEG coated gold sensors. As control BSA from NEB was used. BSA from Sigma was almost completely washed out. Thus, single steps RCA reactions of 0.1 pmol initial template or without template (control) were loaded on PLL(25)-g-PEG(2) coated gold sensors. However, although background signal was significantly reduced from 5.5 ± 1.2 $*10^{-6}$ to 1.34 ± 0.2 $*10^{-6}$ (N=2) for the negative control concerning dissipation changes and from 223 ± 82 Hz to 76 ± 2 Hz (N=2) as concern frequency changes, 0.1 pmol did not distinguished from negative control.

3.2.2 B) Acoustic detection of RCA on neutravidin coated gold sensors

In order to achieve specific absorption of the RCA product on the gold sensor the rest experiments were performed using the biotin-neutravidin interaction as an immobilization method. In that case, single-step RCA reactions with T4 DNA Ligase were conducted in presence of b-dUTP, so that the latter to be incorporated in few sites at the amplified product instead of dTTP. Then, the whole reactions were loaded on neutarvidin-coated gold sensors. Binding to the gold sensor is supposed to be achieved through the interaction of incorporated biotin molecules with neautravidin. **Figure 23** shows the real time addition of neutravidin monitored at 35 MHz. The absorption of neutravidin protein on the gold electrode was verified by typically detecting ΔF ≈ -400 Hz, ΔD ≈ +2 * 10^{-6} at the 35 MHz overtone and 0.003 -0.006 concerning the acoustic ratio. As it summarizes in table 3, a set of factors was investigated so to achieve the best binding on the sensor's surface.

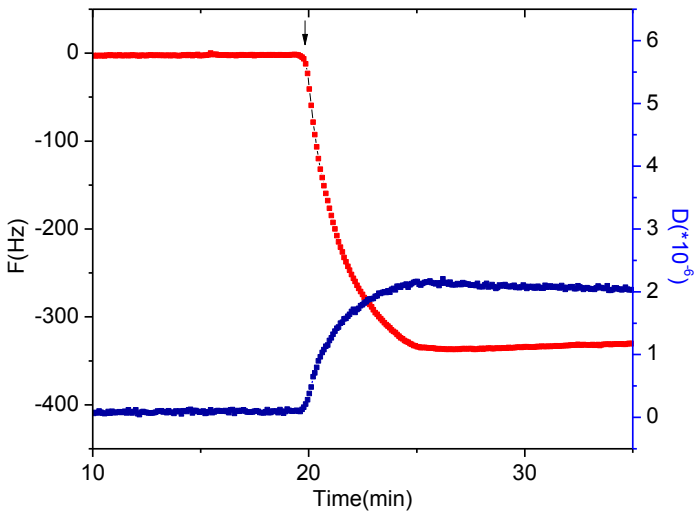

Figure 23: Real time absorption of neutravidin on gold sensors monitored at 35 MHz. Red and blue line depict changes in frequency and energy disssipation respectively. Black arrow indicate the time point were neutravidin touches the sensor's surface.

- **RCA on neutravidin in continuous flow of PBS – $MgCl_2$, pH 7.4**

In these set of experiments, single-step RCA reactions were conducted with 1 pmol, 0.1 pmol and 10 fmol of miRNA-21 as initial target or without template (negative control), in presence of (the minimal amount of) 1/100 b-dUTP compare to dTTP. The reactions were incubated for 30' at RT followed by addition on neutravidin coated gold sensors. The whole acoustic experiment was performed in a continuous flow of buffer PBS – $MgCl_2$ (150 mM and 10 mM respectively), pH 7.4. However, after the addition of sample which was followed by buffer rinsing, the signal never reached a plateau, contrariwise it keeps washing-off. So, in every experiment, changes in frequency and dissipation were measured before the addition of sample and exactly 19 minutes after the sample reached the surface. The bar-graphs in **Figure 24** represent the changes in dissipation and frequency. Only the reactions of 1 pmol initial target are clearly distinguish from the negative control, and only as concern the ΔD. The average values for 1 pmol, 0.1 pmol, 10 fmol and control were 2.8 ± 0.6 $*10^{-6}$, 1.8 ± 0.1 $*10^{-6}$, 2 ± 0.34 $*10^{-6}$ and 1.5 ± 0.58 $*10^{-6}$ respectively.

With purpose to achieve a better LOD on the sensor, it was firstly increased the incubation time from 30' to 60 min at RT. Only the detection of 0.1 pmol as initial template was tested. However, positive reactions continue to not distinguish from negative control. Furthermore, the 60' positive and negative reactions seem to have no difference from the corresponding 30' reactions. Changes in Dissipation are represented in **Figure 24C**.

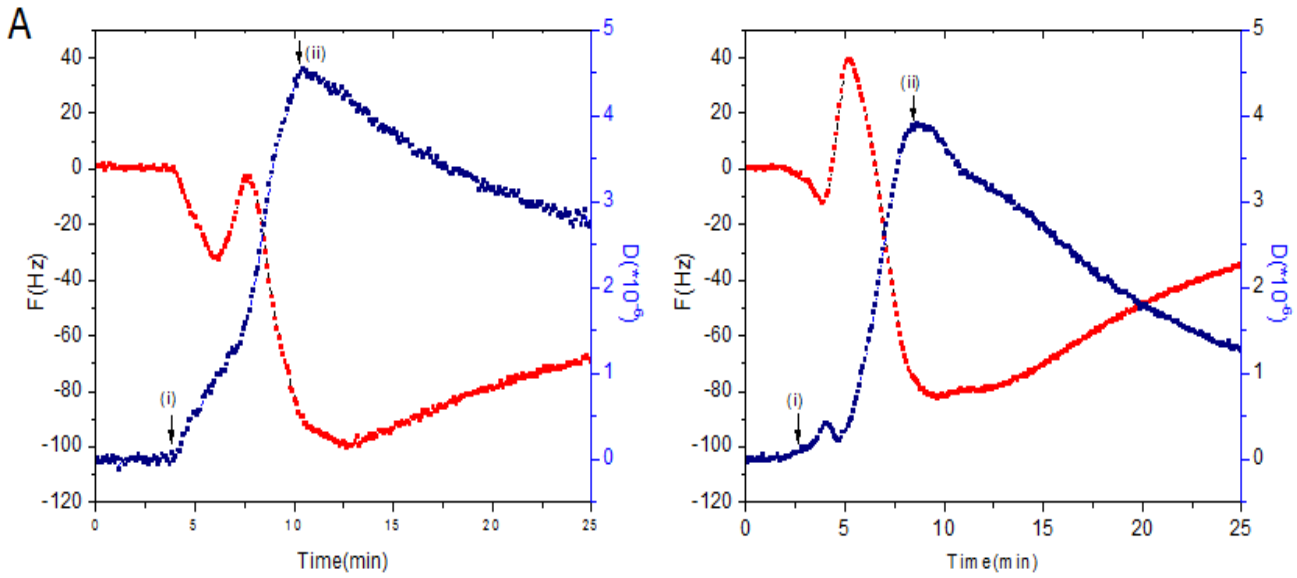

B

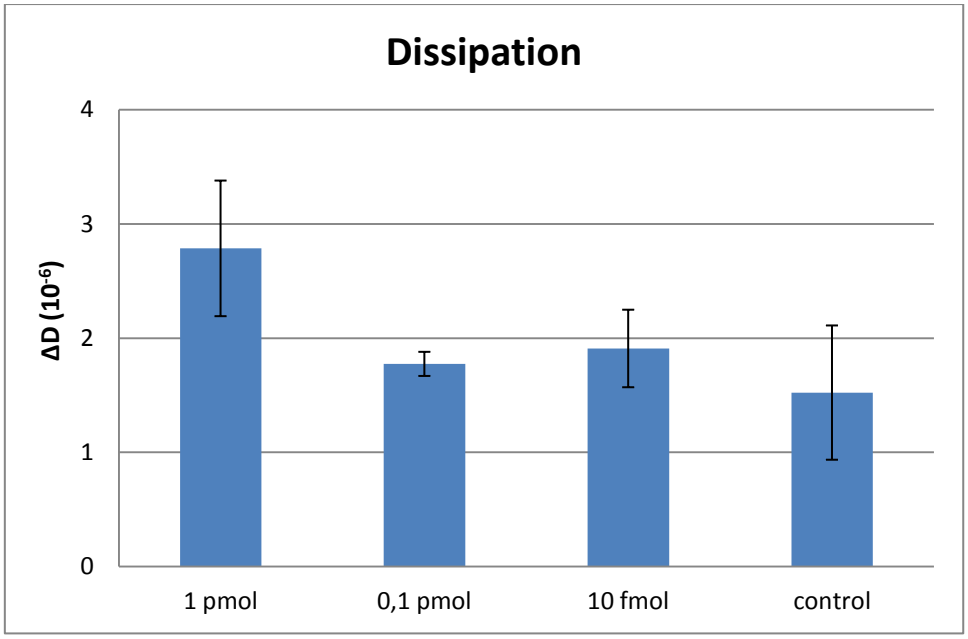
Dissipation
ΔD (10-6)
4
3
2
1
0
1 pmol
0,1 pmol
10 fmol
control

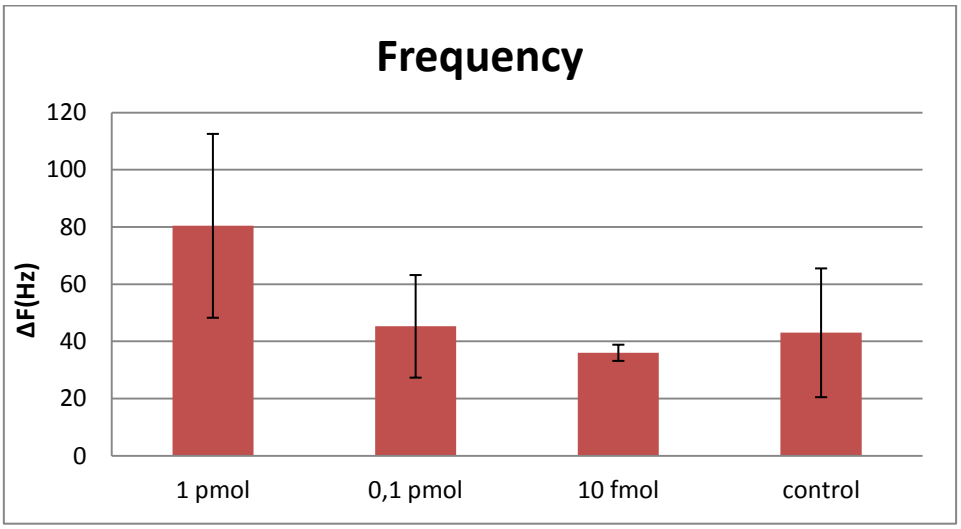
Frequency
ΔF(Hz)
120
100
80
60
40
20
0
1 pmol
0,1 pmol
10 fmol
control

C

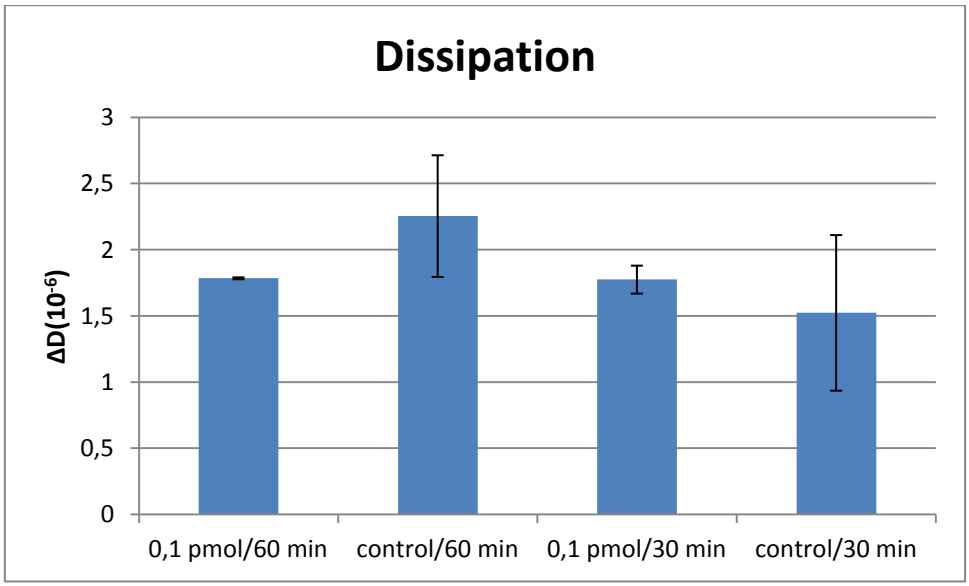
Dissipation
ΔD(10-6)
3
2,5
2
1,5
1
0,5
0
0,1 pmol/60 min
control/60 min
0,1 pmol/30 min
control/30 min

Figure 24: Acoustic detection of biotinylated-RCA on neutravidin in continuous flow of PBS-$MgCl_2$. RCA reactions contain 1/100 b-dUTP compare to dTTP.
A) Real time acoustic curves of frequency (red line) and dissipation (blue line) changes monitored at 35 MHz for 1 pmol (left) and negative (right) reaction. Black arrows indicate the time points where the sample (i) and buffer (ii) touch the surface. **B)** Bar graphs represent the changes in Dissipation and Frequency for positive (1 pmol N = 3, 0.1 pmol N = 6, 10 fmol N= 2) and negative (w/o template, N = 8) reactions incubated for 30 minutes or **C)** 60 minutes at RT (N = 2 for positive and negative control. Only the changes in Dissipation are presented). *N = Number of experiments.

Additional to the incubation time, b-dUTP was also increased from 1/100 to 1/10 compare to dTTP, so more b-dUTP to be incorporated in the amplified product. This time dissipation changes were measured before the addition of sample and both a) in peaks and b) exactly 16 minutes after the sample reached the surface. In both cases, 0.1 pmol was distinguished from negative control. The average values were 4 ± 0.58 $*10^{-6}$ and 3 ± 0.13 $*10^{-6}$ for positive and negative in peaks and 1.7 ± 0.22 $*10^{-6}$ and 1 ± 0.1 $*10^{-6}$ for positive and negative in plateau, respectively **(Figure 25)**.

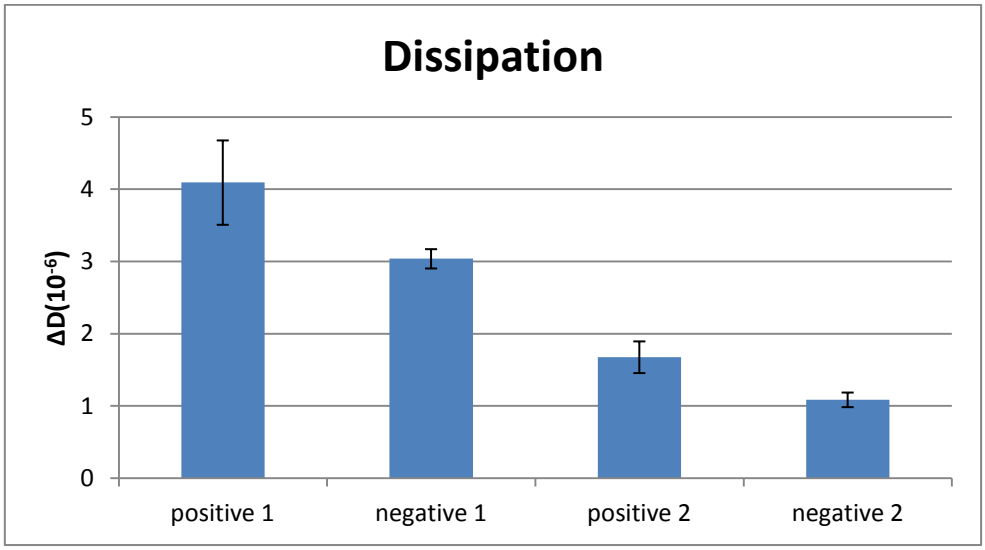

Figure 25: Acoustic detection of 0.1 pmol biotinylated-RCA on neutravidin in continuous flow of PBS-$MgCl_2$. RCA reactions contain 1/10 b-dUTP compare to dTTP.
Bar graphs represent the changes in Dissipation for positive (0.1 pmol) and negative (w/o template) reactions incubated for 60 minutes at RT. Measurements were performed before the addition of sample and both a) in **peaks (positive 1 / negative 1)** and b) and **washing-off phase (positive 2 / negative 2)**. (N = 4 for positive and negative control, * N = Number of experiments)

However, control values were decreased compare to the other two cases. This maybe is due to the effect of the free b-dUTP on the neutravidin sites and how this affects the interaction of neutravidin protein with the other materials of the reaction.

- **RCA on neutravidin in continuous flow of buffer Tris, pH 7.5**

The fact that during the experiments with PBS, after the addition of sample and the buffer rinsing the real time signal never reached a plateau made difficult to say for sure that there was a real binding of the product on neutravidin. So, in order to obtain more clear results and better binding of the RCA product on neutravidin, an extra set of experiments were performed. It was investigated the conduction of the acoustic experiment in the continuous flow of buffer Tris 20 mM, pH 7.5, without any addition of salt. Like before, single step RCA was performed with 0.1 pmol miRNA-21-5p (and w/o target as negative control) and 1/10 b-dUTP compare to dTTP. Reactions were incubated at RT for 60' followed by addition on neutravidin coated sensors. Real time curves are presented in **Figure 26**. Concerning the real time curve which monitors the changes in dissipation (blue line), a 1st peak is created when the **sample** attached to the surface (as always) and a 2nd peak is also created when the **buffer** (of the washing phase that follows) reaches the surface. Then the signal is allowed to reach a plateau. Concerning the real time changes in frequency (red line) a 1st peak is created with the signal going to more negative values when the **sample** attaches the surface (as always). However, when buffer reaches the surface a 2nd peak was created, with the signal going to the positive direction and finally reaching plateau in more positive values than it was before the addition of sample.

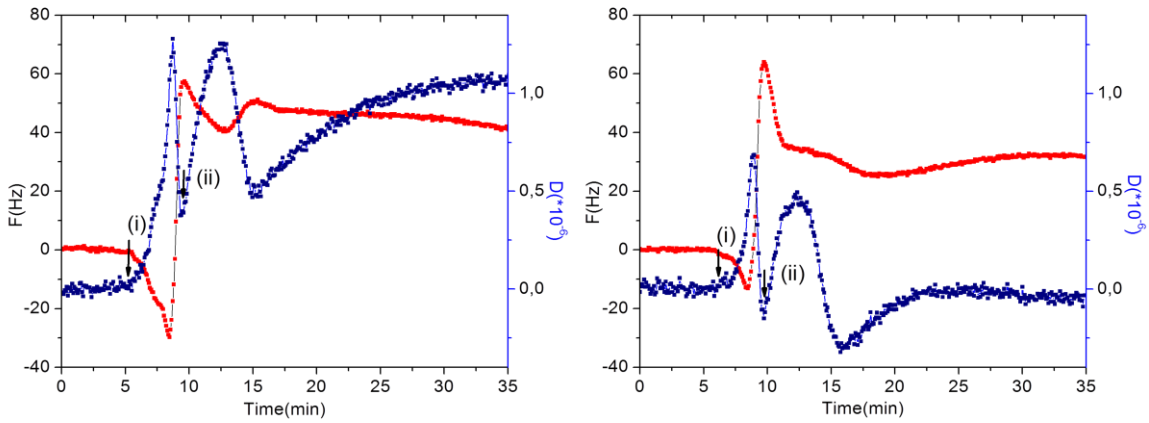

Figure 26: Real time curves monitored upon biotinylated-RCA addition on neutravidin in continuous flow of Tris. RCA reactions contain 1/10 b-dUTP compare to dTTP.
Real time curves of frequency (red line) and dissipation (blue line) changes monitored at 35 MHz for 0.1 pmol (left) and negative (right) reaction. Black arrows indicate the time points where the sample (i) and subsequently the buffer (ii) touch the sensing area.

Changes in frequency and dissipation were measured in every case before the addition of sample and a) at 1st peak, b) 2nd peak and c) plateau. **Figure 27 A & B** represent the changes in dissipation in plateau (A) and 1st and 2nd peaks (B) respectively. 0.1 pmol is distinguished from negative control both in measurements that performed in plateau and 2nd peak. It is worth noting that $\Delta D_{plateau}$ is equal to 0 for the negative and average value for positive is 0.6 ± 0.3 $*10^{-6}$.

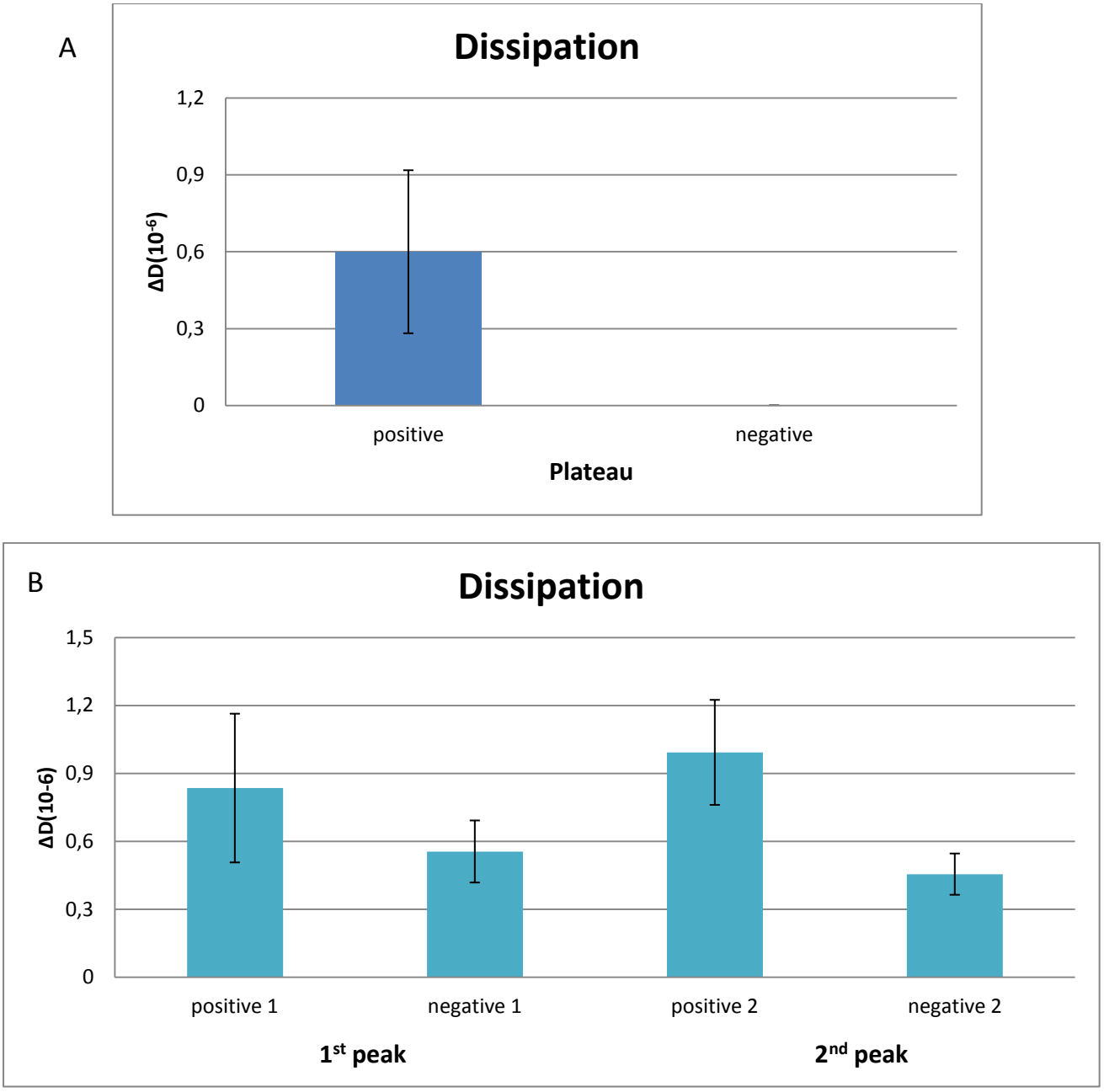

Figure 27: Acoustic detection of 0.1 pmol biotinylated-RCA on neutravidin in continuous flow of Tris. RCA reactions contain b-dUTP in a ratio of 1/10 compare to dTTP.
Bar graphs represent the changes in dissipation for positive (0.1 pmol) and negative (w/o template) reactions incubated for 60 minutes at RT. Measurements were obtained before the addition of sample and: **A)** from plateau (positive / negative) after the washing-off phase was complete **B)** from 1st (positive 1 / negative 1) and 2nd (positive 2/ negative 2) peak. (N = 4 for positive and negative control, * N = Number of experiments)

About the changes in frequency, only in the case where ΔF was measured according the 1st peak, positive distinguished from the control (even though standard deviations error bars are very close to overlap) **(Figure 28)**.

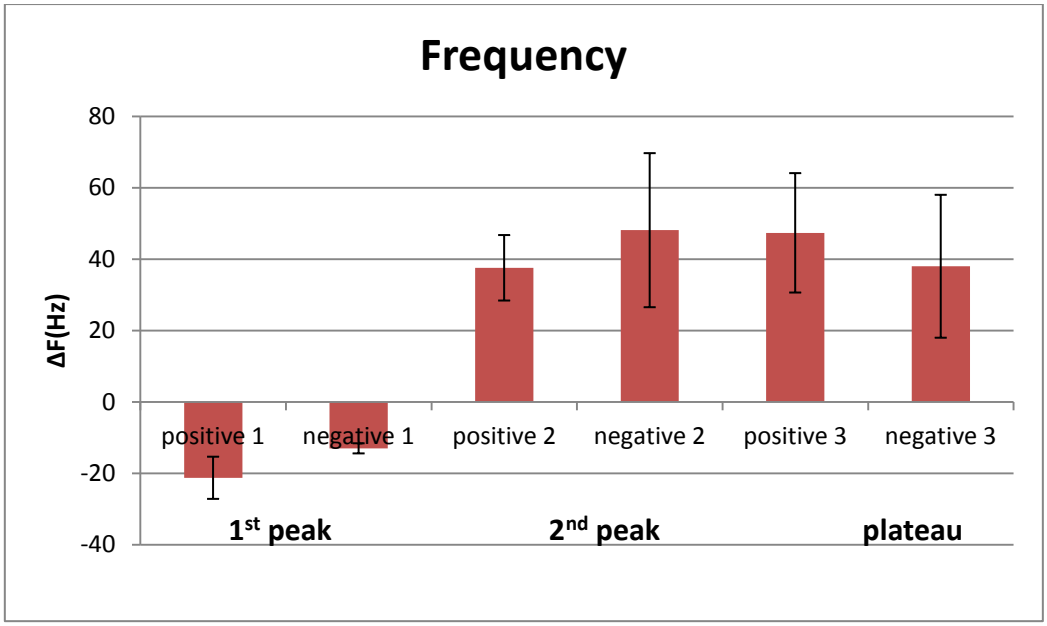

Figure 28: Comparison of frequency changes after the addition of biotinylated-RCA on neutravidin in continuous flow of Tris. RCA reactions contain b-dUTP in a ratio of 1/10 compare to dTTP.

Bar graphs represent the changes in frequency for positive (0.1 pmol) and negative (w/o template) reactions incubated for 60 minutes at RT. Measurements were obtained before the addition of sample and i) from 1st peak (positive 1/ negative 1), 2nd peak (positive 2/ negative 2), and from plateau, after the washing-off phase was complete (positive 3 / negative 3. (N = 4 for positive and negative control, * N = Number of experiments)

Since the acoustic detection of 0.1 pmol RCA reactions has been achieved in both buffers next step was the decreased of LOD from 0.1 pmol to 10 fmol. Again single step reactions of 10 fmol miRNA-21-5p as initial target were incubated for 2.5 and 3.5 hours in presence of 1/10 b-dUTP compare to dTTP. Then, the reactions were loaded on neutravidin coated sensors. Measurements in dissipation and frequency were performed as it was previously described. Both after 2.5 and 3.5 hours of incubation positive reactions did not distinguish from negative **(Figure 29)**. However, in both cases in some experiments the negative controls values have bigger dissipation changes compare to negative control of 60' incubation **(Figure 27 & Figure 29A)**. Maybe, small amount of unspecific product is produced. It is worth noting, that as it seems from **Figure 29C** and standard deviations error bars there was a big variation in real time curve between different experiment repeats after the addition of sample mainly in 1st and 2nd peak creation.

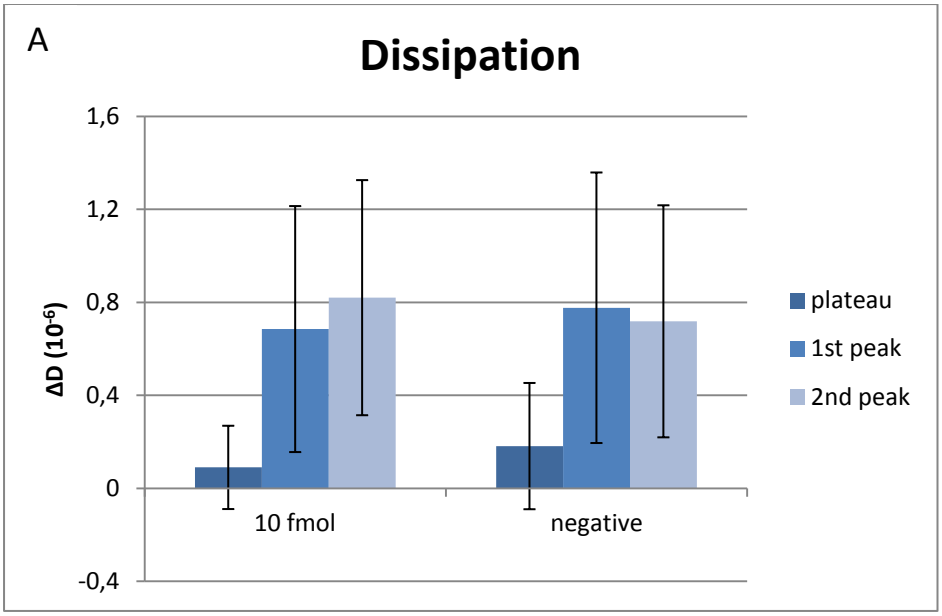

DISSIPATION (ΔD)	
10 fmol	Negative
plateau	plateau
0,1	0,07
0,06	0,24
0,23	0,29
0,35	0,49
-0,1	0,3
-0,1	-0,3

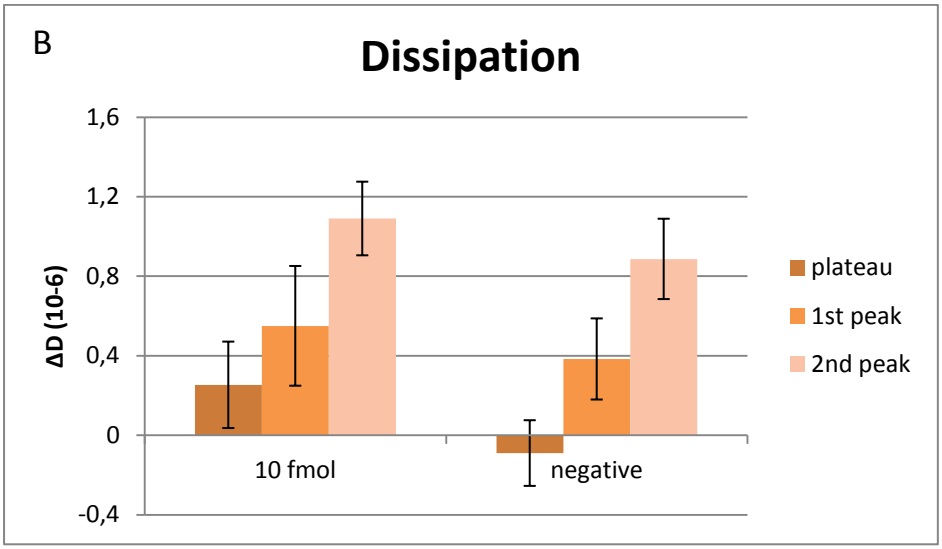

DISSIPATION (ΔD)	
10 fmol	Negative
plateau	plateau
0,29	0,1
0,45	-0,17
0,02	-0,2

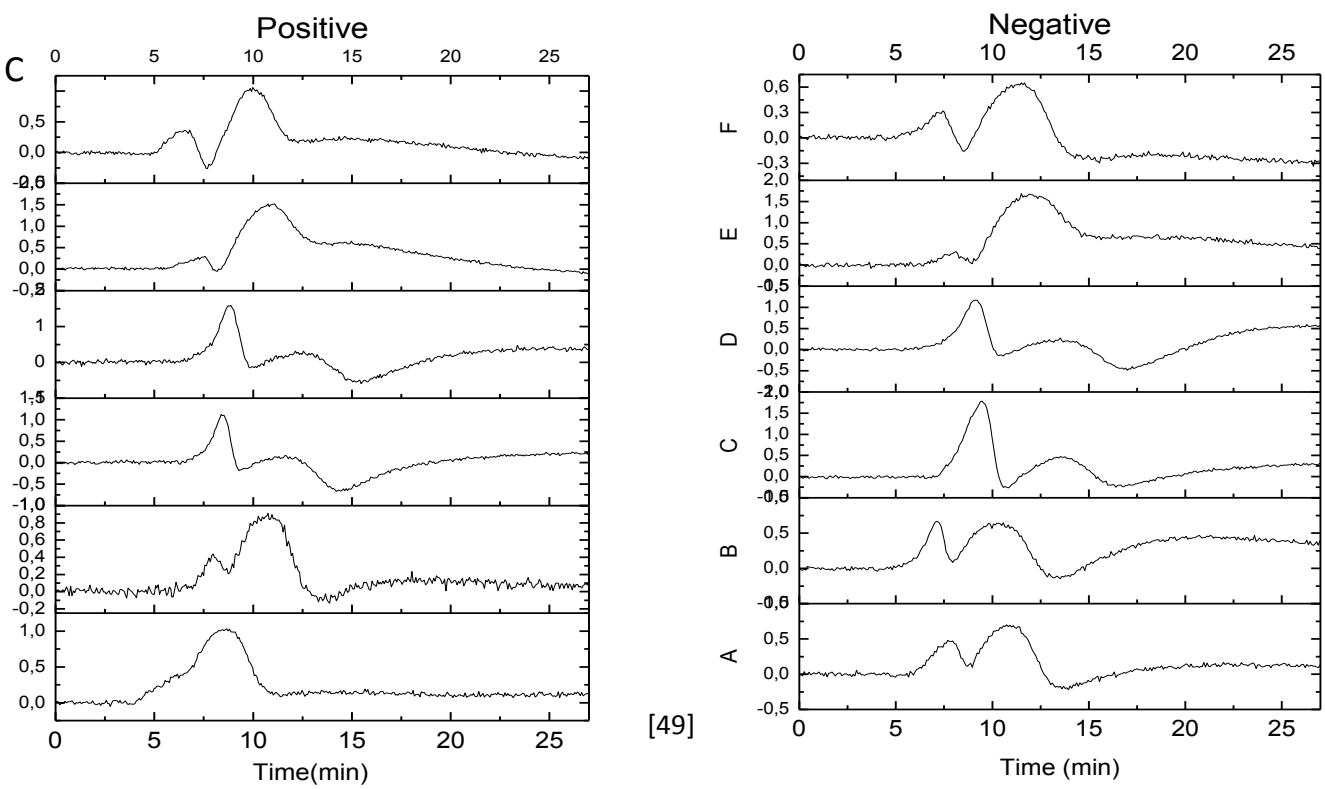

[49]

Figure 29: Acoustic detection of 10 fmol biotinylated-RCA incubated on neutravidin in continuous flow of Tris. RCA reactions contain b-dUTP in a ratio of 1/10 compare to dTTP.
Bar graphs represent the changes in dissipation of 10 fmol and negative (w/o template) reactions incubated for **A)** 2.5 hours and **B)** 3.5 hours at RT. Measurements were obtained before the addition of sample and: i) from plateau after the washing-off phase was complete as well as from ii) 1st and 2nd peak. (N = 6 for 2.5 h & N = 3 for 3.5 h, * N = Number of experiments). **C)** Variation of real time curves between different experiment repeats (**E – F)** after the addition of sample.

- **RCA on neutravidin in continuous flow of buffer MES, pH 5.5**

Finally, a last set of experiments was performed again for the detection of RCA product, emerged from 0.1 pmol miRNA-21-5p as initial target, on neutravidin. This time it was tested the effect of different ionic strength. Since at pH 7.5 both neutravidin and DNA are partly negatively charged (the IP of neutravidin and ssDNA is 6.3 and 4.0-4.5, respectively), it was investigated the binding of biotinylated RCA product on neutravidin at pH 5.5, hoping that it would be pushed the adsorption and binding of RCA due to electrostatic interactions. So, 60' single step RCA reactions were performed with 0.1 pmol miRNA-21-5p (and w/o target as negative control) and 1/10 b-dUTP compare to dTTP, followed by addition on neutravidin coated sensors. The whole acoustic experiment was conducted in continuous flow of buffer MES 45 mM, pH 5.5. **Figure 30A** represents the real time curves of changes in frequency (huge drift is caused after sample's addition) and dissipation and only changes in dissipation are presented in **figure 30B**. Positive reactions did not distinguish from negative. The average values as concern the changes in dissipation were 2.85 ± 0.77 $*10^{-6}$ and 2.57 ± 1.87 $*10^{-6}$ respectively. It is very possible, that pH change caused un-specific absorption on neutarvidin.

A

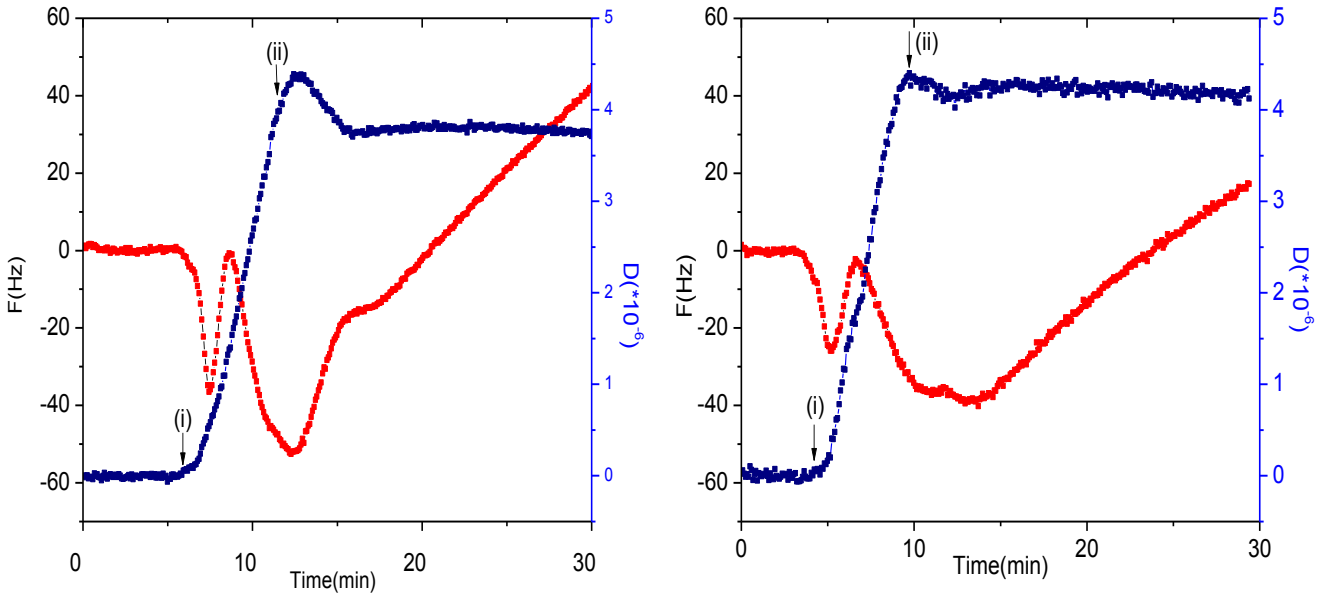

B

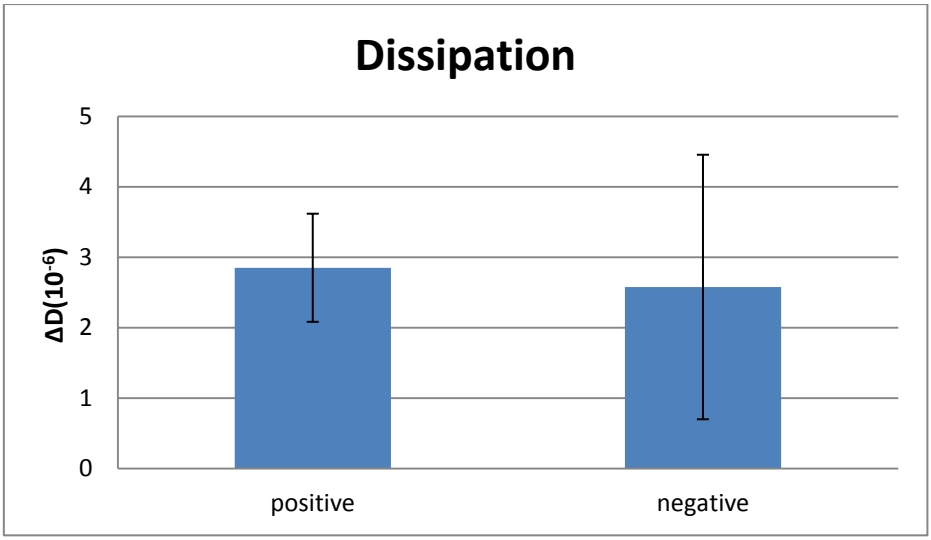

Figure 30: Acoustic detection of biotinylated-RCA on neutravidin in continuous flow of MES, pH 5.5. RCA reactions contain 1/10 b-dUTP compare to dTTP.
A) Real time curves of frequency (red line) and dissipation (blue line) changes monitored at 35 MHz for 0.1 pmol (left) and negative (right) reactions, incubated for 60' at RT. Black arrows indicate the time points where the sample (i) reaches the sensor's surface followed by buffer rinsing (i). **B)** Bar graphs represent the changes in dissipation for positive (0.1 pmol) and negative (w/o template) reactions. Measurements were performed before and after the addition of sample, when the washing-off phase was complete (N = 4 for positive and negative control reactions, * N = Number of experiments)

3.2.2 C) Investigating the effect of free b-dUTP

As concern the part of the experiments where neutravidin-biotin interaction was used as immobilization method for the RCA product, the main problem seemed to be the inability of the incorporated biotins to interact with their binding sites on neutravidin. The most likely and powerful explanation was the existence of competition for neutravidin active sites between the free (non-incorporated) b-dUTP and the biotinylated RCA product. Non-incorporated b-dUTP interacts first with neutravidin binding sites preventing the binding of RCA. The effect of free-b-dUTPs to the binding of b-RCA product during an acoustic experiment was investigated as follows:

- 400 nM or 40 μM (is the amount of b-dUTP in a usual 25 μL reaction with 1/100 or 1/10 b-dUTP compare to dTTP) or no b-dUTP were firstly added on neutravidin coated gold sensors, followed by buffer rinsing exactly like the usual acoustic experiment. Then, 200 pmol (correspond to 1.32 μg) of ss DNA oligonucleotide 20 nt in length carrying a biotin molecule on its 5'end were added on the surface. The experiment was conducted in continuous flow of buffer PBS-$MgCl_2$.

Graph 31 represents the real time curves monitored upon loading **(A)** or not **(B)** of b-dUTP followed by the addition of 200 pmol ss DNA oligo.

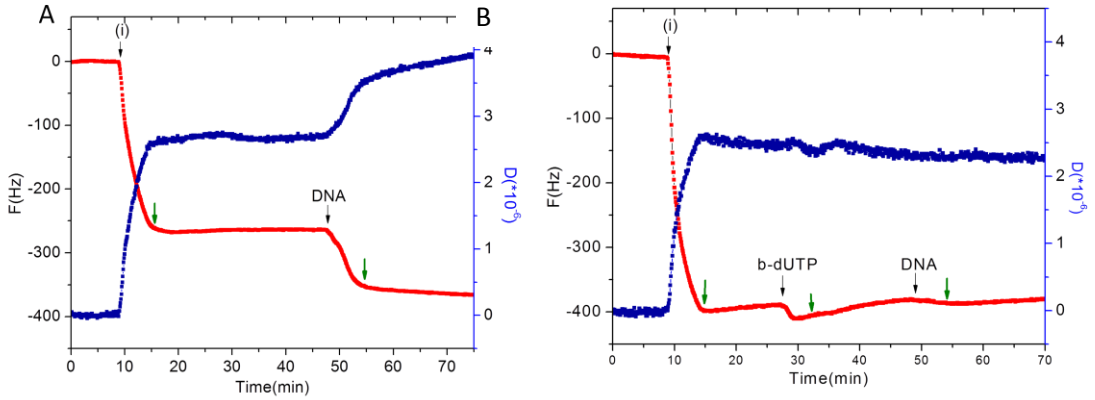

Figure 31: Real time curves monitored upon loading (A) or not (B) of b-dUTP followed by the addition of 200 pmol biotinylated ss DNA oligo.
Real time curves of frequency (red line) and dissipation (blue line) changes monitored at 35 MHz. All steps are presented: addition of nrutarvidin followed by addition of b-dUTP and/or DNA. Black arrows indicate the time points where neutravidin (i) and b-dUTP or DNA (200 pmol b- ss DNA oligo) reached and immobilized on the sensing area, while green arrows indicate the time points where buffer reach the sensor surface.

Without addition of b-dUTP the values of frequency and dissipation changes were 96 Hz and 0.98 $*10^{-6}$ respectively. However, the corresponding values were decreased to 19 Hz/ 0.22 $*10^{-6}$ and 12 Hz/ 0.19 $0*10^{-6}$ if 400 nM or 40 μM of b-dUTP has firstly been added **(Graph 24)**. The above results prove that about 80 % of the available neutravidin binding sites are blocking from b-dUTP.

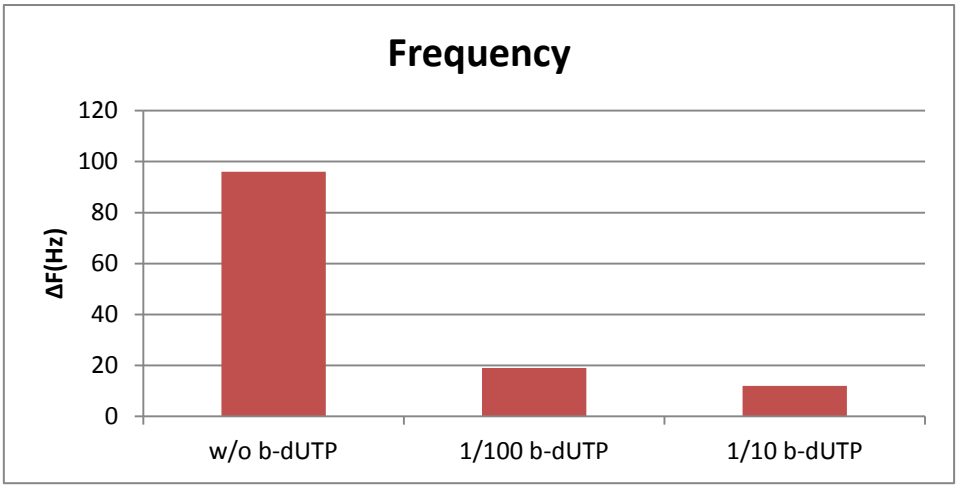

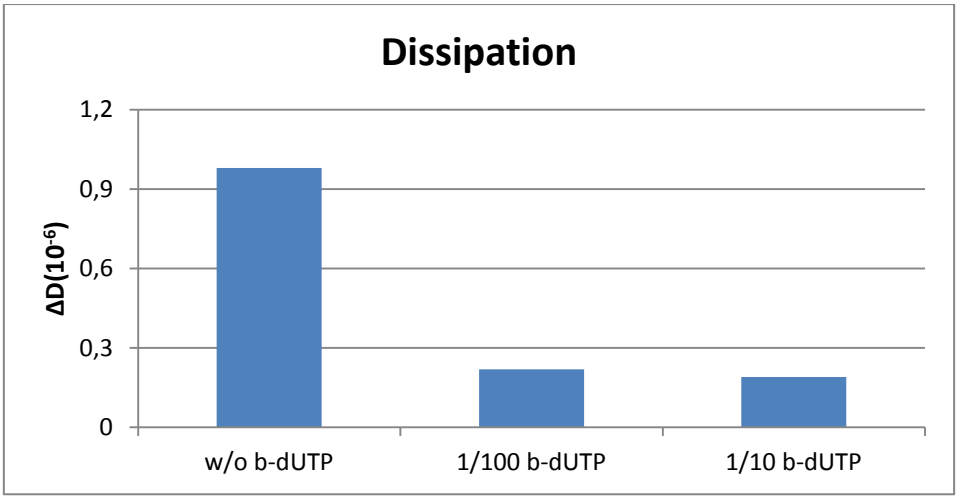

Figure 32: Schematic overview of b-dUTP effect

Bar graphs represent the frequency and dissipation changes after the addition of 200 pmol biotinylated ss DNA oligo on neutravidin coated gold sensors, on which had firstly added 400 nM (1/100 b-dUTP), 40 µM (1/10 b-dUTP) or no (w/o b-dUTP) b-dUTP.

4. Discussion

Cancer is the leading cause of death worldwide. The best way to achieved effective and efficient management of cancer patients is the early diagnosis and the frequent monitoring of patient response to treatment[1]. In this study, It was aimed the development of novel, easy and fast methods for sensitive and efficient detection of a) circulating tumor DNA point mutations and b) circulating miRNA-21 both based on the combined use of QCM acoustic biosensor with RCA DNA amplification method.

4.1 ctDNA

As concern the method for detection of ctDNA point mutations, two chemically synthesized DNA targets, of 85 bp (double-stranded) and 21 nt (single stranded), mimicking ctDNA which carries the KRAS G12D point mutation were used, as well as two different DNA ligases, AmpLigase and T7 DNA Ligase.

T7 DNA ligase shows increased specificity, since the reaction was incubated no more than 30'. Non-specific RCA was probably due to self-ligation of the padlock probe and can be avoided by separating the ligation from the amplification step. Furthermore, it was noticed that during single step reaction use of one instead of two primers leads to better RCA production. This can be due to the different rate that phi29 and T7 DNA liagse act on DNA. In other words, probably phi29 DNA polymerase which has a polymerization rate about 50 nt/sec, displaces T7 DNA ligase before ligation of padlock probe is completed.

On the other hand, an extremely low number of approximately 10 copies of dsDNA target were detected with high specificity within 30 min of RCA reaction by performing a cycling protocol of denaturation and ligation with AmpLigase, enhanced the creation of minicircles and subsequently the template for RCA.

Finally, RCA product of 1 pmol initial target, amplified within 90 min performing a cycling protocol and RCA, was detected with high specificity on QCM-D biosensor via absorption on PLL(25)-*g*-PEG(2) polymer. In the previous studies of Yao et al., 2013[64] and Kordas et al., 2016[65] acoustic detection of RCA product has been performed on QCM and SAW biosensor respectively. The detection was based on ΔF and acoustic ratio (ΔA/ΔPh), in respect. Herein, most clear results were obtained comparing changes in ΔD. However, much more experiments should be performed in order to investigate the detection of lower initial amount of mutant target (ie the 10 copies) diluted in a high ratio of wild type to mutant alleles.

4.2 Circulating miRNA

Concerning the second case, altered levels of miRNA-21 have been associated with multiple diseases, including cancer. Yanzhao Li et al., quantified the levels of miRNA-21 in blood via RT-PCR in both lung cancer patients and healthy people to about 270 and 100 pM, respectively. Although, L-RCA has been widely used for miRNA detection ligation of padlock probe was conducted in a separate reaction prior to RCA. In this study, during a first set of experiments 40 and 400 pM of

miRNA-21 were detected in gel after single step reaction using T4 DNA Ligase and phi29 DNA polymerase at RT, **without** using any heat or other device. Incubation time was about 120 min and 60 min respectively, and a larger amount of amplified product was created without the addition of primer supporting the previous theory about the catalytic rate of phi29 and DNA Ligase. No visualized products from auto-ligation of padlock probe were detected. However, T4 DNA ligase was not able to discriminate the existence of mismatch like T7 and Amp Ligases. Such problem could maybe overcome using T4 RNA ligase 2; T4 RNA ligase 2 is active on RNA:DNA hybrids and exhibit high specificity concerning mismatches near ligation site[45].

About the acoustic detection using QCM-D device, only 1 pmol of miRNA 21 was managed to be detected at RT, and distinguished from control reaction, via absorption on PLL(25)-*g*-PEG(2), comparing changes in dissipation. However, in these set of experiments higher dissipation and frequency changes were obtained with high standard deviation values. It was shown that the so high and so different ΔD and ΔF values were due to the effect of reaction buffers, the enzymes and the large amount of BSA (2.5 μg) contained in the reaction which were non-specifically bound on PLL-*g*-PEG. When it was tested to reduce the addition of BSA per reaction from 2.5 μg to 1 μg combined with BSA purchased from different company (Sigma, fraction V, lyophilized, Sigma, BSA was almost completely washed out. BSA from NEB differentiated from BSA from Sigma that contained 5 % of glycerol, EDTA, KPO4. Glycerol is washed out and the big difference in ΔF and ΔD may is because BSA from NEB has formed aggregates. Moreover, in the case of of T4-RCA reaction, the whole reaction was loaded in each case and not only the 17 μL of the 25 μL. Thinking the results of the KRAS G12D RCA on PLL-g-PEG, first of all 15 of 25 μL of the final reaction was submitted in cycling up to 65 ^{o}C - 95 ^{o}C (this constitutes the first step of 2-step reaction with AmpLigase). This means that both the ligase and the largest amount of BSA were fully denatured. Secondly, during the second step, phi29 was heat inactivated by incubation at 65 ^{o}C. Thirdly, exactly the half amount of both Ligase and phi29 were added in those reactions compare with the T4 - single step reaction of the case here.

As already stated, the ability of PLL(25)-g-PEG(2) and PLL(25)-g-PEG(5) to absorb DNA in a protein resistant manner have been investigated previously in the lab. Better results were obtained about PLL(25)-g-PEG(2), however as concern dsDNA of 635 bp in length after PCR amplification and not ssDNA of thousands nt in length. dsDNA is more negatively charged compare to ssDNA, due to the double sugar phosphate backbone[68], thus dsDNA exhibit higher affinity for the negatively charged PLL-g-PEG. Converting single-stranded RCA product to double-stranded by conducted BRCA or HRCA just via addition of second and third primer complementary to RCA product using the same protocol, will not only increase amplification signal, but also the electrostatic attraction on PLL-g-PEG[44,46].

Alongside, an alternative immobilization method of RCA product on the sensor surface was tested; via neutravidin-biotin interaction, similarly to Kordas et al., 2016[65]. It was achieved the detection of RCA reactions of 0.1 pmol initial target comparing changes in ΔD in two different ways; in the continuous flow of a. PBS-$MgCl_2$ pH 7.4 and b. Tris buffer pH 7.5.

As concern the 2nd case, following the addition of sample and as monitored the changes in dissipation, a 1st peak was created when the **sample** attached to the surface (as always) and a 2nd peak was generated, too, exactly when the **buffer** (of the washing phase that follows) reaches the sensor. The generation of the second peak, when the buffer reaches the surface, could be due to steric rearrangement, as buffer contains no salt (NaCl, PBS) or cations (like Mg^{2+}).

When neutravidin-biotin interaction was used as immobilization method for the RCA product it was proved that there was competition for neutravidin active sites between the free (non-incorporated) b-dUTP and the biotinylated RCA product; up to 80 % of the available neutravidin-binding sites were blocking from free b-dUTP.

A different approach should be designed and used in order to overcome this problem. For example, RCA product could be bound on neutravidin via immobilized biotinylated "capture" probe of the same length with padlock probes (about 70 nt) complementary to single strand RCA product, avoiding the addition of biotin-dUTPs in the reaction. Furthermore, incubation time could be optimized in order to be produced smaller ssDNA RCA products of about 1-2 kb and not 10 of thousands kb. Phi29 can add up to 50nt/sec, in optimal conditions (30 ^{o}C, in presence of SSB protein)[69]. However, in our case the reaction will be conducted at 25 ^{o}C, where phi29 replicated at slower rates, without added SSB protein and maybe there will be a competition with T4 DNA Ligase. 10 minutes could be a good incubation time to start with, as it is also enough for T4 DNA Ligase. Creation of smaller RCA products, combined with the appropriate buffer (salt, Mg^{2+}) would be decreased a lot the entanglement between different RCA products or even of the same long molecule, thus eliminating the steric hindrance on hybridization between RCA products and immobilized biotinylated probes. As a result there will be parts of dsDNA and ssDNA, and may better frequency and dissipation changes will be monitored on QCM biosensor, proportional of the amount of initial target.

5. Concluding Remarks and future perspectives

In this work, it was aimed the development of novel, easy and fast methods, suitable in clinical application, for sensitive and efficient detection of a) circulating tumor DNA point mutations and b) circulating miRNAs both based on the combined use of QCM acoustic biosensor with RCA DNA amplification method. In both cases, various methods were tested and the whole procedure needs better optimization and design. However, the fact that it was managed to combine the ligation and amplification procedure into one single-step for the first time, and most importantly at RT without using any machine as well as the applicability of RCA directly in serum[41,42] or in saliva[70] is very promising as it may allow further integration with microfluidics in order to design Point-of-Care system for miRNA detection. Concluding, both methods could treat like promising approaches for the development of novel biosensing platforms for Liquid biopsy and cancer monitoring.

6. References

1. Larrea, E. *et al.* New Concepts in Cancer Biomarkers : Circulating miRNAs in Liquid Biopsies. (2016). doi:10.3390/ijms17050627

2. Wang, Z. H. & Xu, C. J. Research Progress of MicroRNA in Early Detection of Ovarian Cancer. **128,** (2015).

3. Endzeli, E. *et al.* Diagnostic , prognostic and predictive value of cell-free miRNAs in prostate cancer : a systematic review. *Mol. Cancer* **15,** 1–13 (2016).

4. Egatz-gomez, A. *et al.* Future microfluidic and nanofluidic modular platforms for nucleic acid liquid biopsy in precision medicine. *Biomicrofluidics* **32902,** (2016).

5. Han, X., Wang, J. & Sun, Y. Circulating Tumor DNA as Biomarkers for Cancer Detection. *Genomics Proteomics Bioinformatics, ELSEVIER* **15,** 59–72 (2017).

6. Ospedale, G. Integrating liquid biopsies into the management of cancer. doi:10.1038/nrclinonc.2017.14

7. Bellassai, N. & Spoto, G. Biosensors for liquid biopsy : circulating nucleic acids to diagnose and treat cancer. *Anal. Bioanal. Chem.* 7255–7264 (2016). doi:10.1007/s00216-016-9806-3

8. Volik, S., Alcaide, M., Morin, R. D. & Collins, C. Cell-free DNA (cfDNA): Clinical Significance and Utility in Cancer Shaped By Emerging Technologies. *Mol. Cancer Res.* **14,** 898–909 (2016).

9. Wan, J. C. M. *et al.* Liquid biopsies come of age: towards implementation of circulating tumour DNA. *Nat. Publ. Gr.* (2017). doi:10.1038/nrc.2017.7

10. Spindler, K. G. Methodological , biological and clinical aspects of circulating free DNA in metastatic colorectal cancer. (2017). doi:10.1080/0284186X.2016.1253861

11. Krishnamurthy, N., Spencer, E., Torkamani, A. & Nicholson, L. Liquid Biopsies for Cancer : Coming to a Patient near You. *Clin. Med. (Northfield. Il).* **6,** 9–11 (2017).

12. Ma, M. *et al.* ‘ Liquid biopsy ’— ctDNA detection with great potential and challenges. *Ann Transl Med* **3,** 1–8 (2015).

13. Li, X. & Zhou, C. Comparison of cross-platform technologies for EGFR T790M testing in patients with non-small cell lung cancer. *Oncotarget* (2017).

14. Hudecova, I. Digital PCR analysis of circulating nucleic acids. *Clin. Biochem.* **48,** 948–956 (2015).

15. Garcı, M. & Olmedillas-lo, S. Current and Emerging Applications of Droplet Digital PCR in Oncology. (2017). doi:10.1007/s40291-017-0278-8

16. Mauger, F. & How-kit, A. COLD-PCR Technologies in the Area of Personalized Medicine : Methodology and Applications. (2017). doi:10.1007/s40291-016-0254-8

17. K, I., Shephard, S. & Candrian, U. Evaluation of the ligase chain reaction (LCR) for the detection of point mutations. **283,** 119–123 (1992).

18. Yi, P., Jiang, H., Li, L. & Dai, F. A New Genotyping Method for Detecting Low Abundance Single Nucleotide Mutations Based on Gap Ligase Chain Reaction and Quantitative PCR Assay. 161–167 (2012). doi:10.1007/s12013-011-9277-2

19. Qi, X., Bakht, S., Devos, K. M., Gale, M. D. & Osbourn, A. L-RCA (ligation-rolling circle amplification): a general method for genotyping of single nucleotide polymorphisms (SNPs). **29,** 1–7 (2001).

20. Zhang, S., Wu, Z., Shen, G. & Yu, R. A label-free strategy for SNP detection with high fidelity and sensitivity based on ligation-rolling circle amplification and intercalating of methylene blue. *Biosens. Bioelectron.* **24,** 3201–3207 (2009).

21. Pickering, J. *et al.* Integration of DNA ligation and rolling circle amplification for the homogeneous , end-point detection of single nucleotide polymorphisms. *Nucleic Acids Res.* **30,** (2002).

22. Jr, L. D. S. L. & Zhou, D. Nano-enabled bioanalytical approaches to ultrasensitive detection of low abundance single nucleotide polymorphisms. *Analyst* **140,** 3872–3887 (2015).

23. Troiano, G. *et al.* Circulating miRNAs from blood , plasma or serum as promising clinical biomarkers in oral squamous cell carcinoma : A systematic review of current findings. **63,** 30–37 (2016).

24. Chakraborty, C. & Das, S. Profiling cell-free and circulating miRNA : a clinical diagnostic tool for different cancers. *Tumor Biol.* (2016). doi:10.1007/s13277-016-4907-3

25. Ortiz-quintero, B. Cell-free microRNAs in blood and other body fluids , as cancer biomarkers. 281–303 (2016). doi:10.1111/cpr.12262

26. Yicheng, Z., Yuanyuan, S., Li, Y., Guangqi, S. & Chunbo, T. Circulating microRNAs: Promising Biomarkers Involved in Several Cancers and Other Diseases. *DNA Cell Biol.* **36,** 1–18 (2017).

27. Mitchell, P. S. *et al.* Circulating microRNAs as stable blood-based markers for cancer detection. (2008).

28. Wang, F. *et al.* Atherosclerosis-Related Circulating miRNAs as Novel and Sensitive Predictors for Acute Myocardial Infarction. **9,** (2014).

29. Churov, A. V, Oleinik, E. K. & Knip, M. MicroRNAs in rheumatoid arthritis : Altered expression and diagnostic potential. *Autoimmun. Rev.* **14,** 1029–1037 (2015).

30. Louten, J., Beach, M., Palermino, K., Weeks, M. & Holenstein, G. MicroRNAs Expressed during Viral Infection : Biomarker Potential and Therapeutic Considerations. **10,** 25–52 (2015).

31. Verma, P., Pandey, R. K., Prajapati, P. & Prajapati, V. K. Circulating MicroRNAs : Potential and Emerging Biomarkers for Diagnosis of Human Infectious Diseases. **7,** 1–7 (2016).

32. Maria, R., Saplacan, M. & Mircea, P. A. MICRORNAS AS NON-INVASIVE SCREENING BIOMARKERS OF COLORECTAL CANCER. *Clujul Med.* **88,** 453–456 (2015).

33. Shan, L. *et al.* Diagnostic value of circulating miR-21 for colorectal cancer : A meta-analysis. **15,** 47–56 (2015).

34. Llano-diez, M. *et al.* Digital PCR quantification of miR-30c and miR-181a as serum biomarkers for Duchenne muscular dystrophy. *Neuromuscul. Disord.* **27,** 15–23 (2017).

35. Shen, Y. *et al.* Amplification-based method for microRNA detection. *Biosens. Bioelectron.* **71,** 322–331 (2015).

36. Kappel, A. & Keller, A. miRNA assays in the clinical laboratory : workflow , detection technologies and automation aspects. **55,** 636–647 (2017).

37. Zheng, X., Niu, L., Wei, D., Li, X. & Zhang, S. Label-free detection of microRNA based on coupling

multiple isothermal amplification techniques. *Nat. Publ. Gr.* 2–7 (2016). doi:10.1038/srep35982

38. Yao, B. O. *et al.* Quantitative analysis of zeptomole microRNAs based on isothermal ramification amplification. 1787–1794 (2009). doi:10.1261/rna.1555209.4

39. Ou, L., Sun, A. & Liu, K. Rolling Circle Amplification-Based Biosensors. *LANL* **48,** 1199–1216 (2017).

40. Tian, T., Wang, J. & Zhou, X. A review : microRNA detection methods. *Org. Biomol. Chem.* **13,** 2226–38 (2015).

41. Cheng-Yi Hong, X. C. Direct detection of circulating microRNAs in serum of cancer patients by coupling protein facilitated specific enrichment and rolling circle amplification. *Chem. Commun* **50,** 3292–3295 (2014).

42. Li, Y., Liang, L. & Zhang, C. Isothermally Sensitive Detection of Serum Circulating miRNAs for Lung Cancer Diagnosis. (2013).

43. Goo, N. & Kim, D. Rolling Circle Amplification as Isothermal Gene Amplification in Molecular Diagnostics. (2016). doi:10.1007/s13206-016-0402-6

44. Ali, M. M. *et al.* Rolling circle amplification: a versatile tool for chemical biology, materials science and medicine. *Chem Soc Rev* 29–37 (2014). doi:10.1039/c3cs60439j

45. Liu, H. *et al.* High Specific and Ultrasensitive Isothermal Detection of MicroRNA by Padlock Probe-Based Exponential Rolling Circle Ampli fi cation. *Anal. Chem.* **85,** 7941–7 (2013).

46. Cheng, Y., Zhang, X., Li, Z., Jiao, X. & Wang, Y. Highly Sensitive Determination of microRNA Using Target-Primed and Branched Rolling-Circle Amplification. *Angew Chem* 3268–3272 (2009). doi:10.1002/anie.200805665

47. Cheng, M. M. *et al.* Nanotechnologies for biomolecular detection and medical diagnostics. (2006). doi:10.1016/j.cbpa.2006.01.006

48. Persano, S. *et al.* Label-Free Isothermal Amplification Assay for Speci fi c and Highly Sensitive Colorimetric miRNA Detection. (2016). doi:10.1021/acsomega.6b00109

49. Graybill, R. M. & Bailey, R. C. Emerging Biosensing Approaches for microRNA Analysis. (2016). doi:10.1021/acs.analchem.5b04679

50. Online, V. A., Johnson, B. N. & Mutharasan, R. Biosensor-based microRNA detection: techniques, design, performance, and challenges. *Analyst* (2014). doi:10.1039/c3an01677c

51. Chang, K., Deng, S. & Chen, M. Novel biosensing methodologies for improving the detection of single nucleotide polymorphism. *Biosens. Bioelectron.* **66,** 297–307 (2015).

52. Bhalla, N., Jolly, P., Formisano, N. & Estrela, P. Introduction to biosensors. 1–8 (2016). doi:10.1042/EBC20150001

53. Svitel, J. & Katrl, J. Optical biosensors. 91–100 (2016). doi:10.1042/EBC20150010

54. Fogel, R., Limson, J. & Seshia, A. A. Acoustic biosensors. 101–110 (2016). doi:10.1042/EBC20150011

55. Hammond, J. L., Formisano, N., Estrela, P., Carrara, S. & Tkac, J. Electrochemical biosensors and nanobiosensors. 69–80 (2016). doi:10.1042/EBC20150008

56. Durmu, N. G. *et al.* Acoustic-Based Biosensors. 1–15 (2014). doi:10.1007/978-3-642-27758-0

57. Vellekoop, M. J. Acoustic wave sensors and their technology. **36,** (1998).

58. Ferreira, G. N. M. & Tome, B. Acoustic wave biosensors : physical models and biological applications of quartz crystal microbalance. 689–697 (2009). doi:10.1016/j.tibtech.2009.09.003

59. Das, J. *et al.* analysis of circulating nucleic acids in serum. *Nat. Chem.* 1–7 (2015). doi:10.1038/nchem.2270

60. Wang, M. *et al.* One-Step, Ultrasensitive, and Electrochemical Assay of microRNAs Based on T7 Exonuclease Assisted Cyclic Enzymatic Ampli fi cation. (2014).

61. Ren, Y., Deng, H., Shen, W. & Gao, Z. A Highly Sensitive and Selective Electrochemical Biosensor for Direct Detection of MicroRNAs in Serum. *Anal. Chem.* (2013).

62. J. Zheng, Dandan Ma, Muling Shia, Junhui Bai, Yinhui Li, J. Y. & Yang, R. A New Enzyme-Free Quadratic SERS Signal Amplification Approach for Circulating MicroRNA Detection in Human Serum. *Chem.Comm.* (2015). doi:10.1039/C5CC06549F

63. Tian, Q. *et al.* Carbon nanotube enhanced label -free detection of microRNAs based on hairpin probe triggered solid-phase rolling-circle amplification. *Nanoscale* (2014). doi:10.1039/c4nr05243a

64. Yao, C., Xiang, Y., Deng, K., Xia, H. & Fu, W. Chemical Sensitive and specific HBV genomic DNA detection using RCA-based QCM biosensor. *Sensors Actuators B. Chem.* **181,** 382–387 (2013).

65. Kordas, A. *et al.* Rapid Salmonella detection using an acoustic wave device combined with the RCA isothermal DNA ampli fi cation method. *SBSR* **11,** 121–127 (2016).

66. Papadakis, G., Palladino, P., Chronaki, D. & Gizeli, E. Sample-to-answer acoustic detection of DNA in complex samples. *Chem. Commun.* **53,** 8058–8061 (2017).

67. Li, Y., Li, W. E. N., Ouyang, Q., Hu, S. & Tang, J. Detection of lung cancer with blood microRNA-21 expression levels in Chinese population. 991–994 (2011). doi:10.3892/ol.2011.351

68. Tan, Z. & Chen, S. Nucleic Acid Helix Stability : Effects of Salt Concentration , Cation Valence and Size , and Chain Length. **90,** (2006).

69. Ducani, C. & Bernardinelli, G. Rolling circle replication requires single-stranded DNA binding protein to avoid termination and production of double-stranded DNA. **42,** 10596–10604 (2014).

70. Zahran, F., Ghalwash, D., Shaker, O. & Scully, C. Salivary microRNAs in oral cancer. 739–747 (2015). doi:10.1111/odi.12340